Fatigue-Damage Estimation and Control for Wind Turbines

Barradas Berglind, Jose de Jesus

DOI (link to publication from Publisher):
10.5278/vbn.phd.engsci.00040

Publication date:
2015

Document Version
Publisher's PDF, also known as Version of record

Link to publication from Aalborg University

Citation for published version (APA):
Barradas Berglind, J. D. J. (2015). *Fatigue-Damage Estimation and Control for Wind Turbines*. Aalborg Universitetsforlag. Ph.d.-serien for Det Teknisk-Naturvidenskabelige Fakultet, Aalborg Universitet https://doi.org/10.5278/vbn.phd.engsci.00040

FATIGUE-DAMAGE ESTIMATION AND CONTROL FOR WIND TURBINES

BY
JOSÉ DE JESÚS BARRADAS BERGLIND

DISSERTATION SUBMITTED 2015

AALBORG UNIVERSITY
DENMARK

José de Jesús Barradas Berglind

Fatigue-Damage Estimation and Control for Wind Turbines

AALBORG UNIVERSITY
DENMARK

Thesis submitted:	October 2015
PhD supervisor:	Professor Rafal Wisniewski Aalborg University
PhD committee:	Professor Zhe Chen (chairman) Aalborg University
	Professor Jacquelien Scherpen University of Groningen
	Associate Professor Jan-Willem van Wingerden Delft University of Technology
PhD Series:	Faculty of Engineering and Science, Aalborg University

ISSN (online): 2246-1248
ISBN (online): 978-87-7112-398-2

Published by:
Aalborg University Press
Skjernvej 4A, 2nd floor
DK – 9220 Aalborg Ø
Phone: +45 99407140
aauf@forlag.aau.dk
forlag.aau.dk

Printed in Denmark by Rosendahls, 2015

List of enclosed publications:

[A] J.J. Barradas-Berglind, and Rafael Wisniewski. "Representation of Fatigue for Wind Turbine Control". *Submitted for publication to Wind Energy*, 2015.

[B] J.J. Barradas-Berglind, Rafael Wisniewski, and Mohsen Soltani. "Fatigue Damage Estimation and Data-based Control for Wind Turbines". *IET Control Theory & Applications, Special issue: Data-based control and process monitoring with industrial applications*, 9(7), pp. 1042–1050, March 2015.

[C] J.J. Barradas-Berglind, Rafael Wisniewski, and Mohsen Soltani. "Fatigue Load Modeling and Control for Wind Turbines based on Hysteresis Operators". *Proceedings of the 2015 American Control Conference (ACC)*, pp. 3721–3727, July 2015.

[D] J.J. Barradas-Berglind, and Rafael Wisniewski. "Control of Linear Systems with Preisach Hysteresis Output with Application to Damage Reduction". *Proceedings of the 14th European Control Conference (ECC) 2015*, pp. 3577-3583, July 2015.

[E] J.J. Barradas-Berglind, Bayu Jayawardhana and Rafael Wisniewski. "Wind Turbine Control with Active Damage Reduction through Energy Dissipation". *Submitted for publication to the 2016 American Control Conference (ACC)*, 2015.

[F] J.J. Barradas-Berglind, Bayu Jayawardhana and Rafael Wisniewski. "Energy Dissipation in Hysteresis Models for Wind Turbine Control Damage Reduction". *Submitted for publication to IEEE Transactions on Control Systems Technology*, 2015.

[G] J.J. Barradas-Berglind, and Rafael Wisniewski. "Wind Farm Axial-Induction Factor Optimization for Power Maximization and Load Alleviation". *Submitted for publication to the 15th European Control Conference (ECC)*, 2015.

This thesis has been submitted for assessment in partial fulfillment of the PhD degree. The thesis is based on the submitted or published scientific papers which are listed above. Parts of the papers are used directly or indirectly in the extended summary of the thesis. As part of the assessment, co-author statements have been made available to the assessment committee and are also available at the Faculty. The thesis is not in its present form acceptable for open publication but only in limited and closed circulation as copyright may not be ensured.

Dedicated to my parents

Contents

Preface

This thesis is submitted as a collection of papers in partial fulfillment of a Ph.D. study at the Section of Automation and Control, Department of Electronic Systems, Aalborg University, Denmark. The work was conducted from November 2012 to October 2015, and was supported by the the Danish Council for Strategic Research under the EDGE —Efficient Distribution of Green Energy— research project.

The thesis consists of two parts. The first part encompasses Chapters 1–4, containing the introduction, motivation, and summary of the contributions, complemented by Chapter 5 that gives the closing remarks. The second part is comprised by the publications enclosed as [Paper A–G], presenting the contributions in detail. The order of the enclosed papers and results largely represents the progression of the work throughout the duration of the study; a special case being [Paper A], which provides a more general view and is therefore presented first.

Besides the layout modification and reformatting, all enclosed publications are presented in the same form as they were published, and thus no modifications have been made to phrasings, structure, notation, etc. An exception to the former are a few minor errata which have been corrected in some of the contributions. Accordingly, footnotes have been inserted to indicate where any changes have been made with respect to the original papers. As no other changes have been made, the notation varies from one paper to another, reflecting the progress and refinement of the work.

José de Jesús Barradas Berglind
Aalborg University, October 2015

Acknowledgements

Three years ago I started a journey that took me to Denmark, and in particular to Aalborg. This journey culminates with this thesis, which contains either directly or indirectly the efforts of many people. Therefore, I would like to thank them here.

First and foremost I would like to thank my supervisor Rafael Wisniewski for his constant support, patience and optimism, for sharing with me his theoretical know-how, for the great out-of-the-box discussions we had, and for giving me leeway while keeping track of the overall picture. I never could have hoped for a better supervisor, my deepest gratitude goes to you Rafael.

I am also greatly indebted to my co-authors, Mohsen Soltani for helping me get started with my first papers and for the practical remarks, and Bayu Jayawardhana for welcoming me during my stay abroad, for providing new insights on my project and for the constructive discussions we had.

Furthermore, my thanks go to the people from the Automation and Control Section at Aalborg University, where the nice and friendly atmosphere made it a very enjoyable workplace. Specially, my gratitude goes to Christoffer Sloth for the late-hour discussions and for his comments on the introduction of this thesis, John Leth for his savvy advice on literature, methods and pool, and Kasper Vinther for the translation of the abstract to Danish and the discussions while we were office mates. As part of my Ph.D. study I had the opportunity to visit the Engineering and Technology Institute Groningen, at the University of Groningen, the Netherlands. I would like to thank everyone there, for making it a successful, interesting and fruitful visit. Also my gratitude goes to Mauricio Muñoz for his help and for proof-reading some of my work.

As special debt of gratitude is also owed to the assessment committee, thank you for agreeing to review my thesis.

Lastly, I would like to acknowledge the encouragement of my family and friends. None of this would have been possible without the ever present support and encouragement of my parents Consuelo and Jesús. Things like my dad making sure I handed in my homework as a kid, and my mom proof-reading most of my manuscripts are just a few examples; this thesis is yours as much as it is mine. In addition, I thank my brother Axel who always lent an ear to my issues despite the distance and a complicated working schedule.

José de Jesús Barradas Berglind
Aalborg University, October 2015

Abstract

Fatigue-damage is a critical factor in structures and materials exposed to harsh operating conditions, both in the design stage and during the control of their operation. This is precisely the case of wind turbines since their operating environment includes turbulent and rapidly changing wind flow conditions. Initially, this thesis addresses and compares the most recognized approaches to estimate the damage caused by fatigue in the component level and their applicability to the control of wind turbines. The underlying relationships between these fatigue estimation methods are also explored and underlined.

The most popular and well-known damage estimation technique amongst those is the so-called rainflow counting. However, since it is based on a counting algorithm, its usability for control purposes is limited. Thus, the following part of this thesis focuses on damage estimation based on hysteresis operators, leaning on the equivalence between rainflow counting, and the variations of a Preisach hysteresis operator. This provides the opportunity to include a damage estimator in the control loop, since hysteresis operators are based on measurements.

Consequently, three different types of control strategies based on hysteresis operators are proposed. The first one is a modified predictive control strategy that incorporates the fatigue estimation via a least-squares interpolation through the cost functional penalties. The second one is a model predictive control strategy formulated in the mixed logical dynamical systems framework, which characterizes the behavior of the discretized Preisach hysteresis in its output. The third strategy incorporates the dissipated energy into the cost functional of the problem as a damage surrogate, transferring the damage and dissipation properties from the Preisach hysteresis to the Duhem hysteresis; the latter having the advantage of being described as a differential equation.

Lastly, a wind farm mixed-objective operation optimization strategy is proposed, allowing the wind farm operator to balance the power production and the wind turbines wear. This is of particular interest when considering wind farm integration with the electricity market.

This work adds to the current insight of fatigue-damage estimation in wind turbine components and how to synthesize control strategies that include hysteresis operators. Furthermore, this work also contributes to address the mixed-objective of wind energy conversion systems, namely, power extraction maximization and mechanical load alleviation.

Resumé

Slitageskader er en kritisk faktor i konstruktioner og materialer, der udsættes for barske driftsbetingelser, både i projekteringsfasen og i kontrol under deres drift. Det er netop tilfældet med vindmøller, da deres driftsmiljø omfatter turbulente og hurtigt skiftende vind flow. Denne afhandling adresserer og sammenligner i første omgang de mest anerkendte tilgange til estimering af skader forårsaget af slid på komponentniveau og ser på deres anvendelighed ifm. kontrol af vindmøller. De underliggende forhold mellem disse metoder for estimering af slid udforskes og understreges også.

Den mest populære og velkendte metode for skadeestimering blandt disse er den såkaldte Rainflow counting. Men dens anvendelighed ifm. kontrol er begrænset, da den er baseret på en optællingsalgoritme. Den resterende del af denne afhandling fokuserer derfor på skadeestimering baseret på hysterese operatører, læner sig op af ækvivalensen mellem Rainflow counting og varianter af en Preisach hysterese operatør. Dette giver mulighed for at inkludere en skadeestimator i reguleringssløjfen, idet hysterese operatører er baseret på målinger.

Derfor foreslås tre forskellige typer af kontrolstrategier baseret på hysterese operatører. Den første er en modificeret prædiktiv kontrolstrategi, der inkorporerer slitageestimering ved hjælp af en mindste kvadraters interpolation igennem vægtninger i kostfunktionen. Den anden er en modelprædiktiv kontrolstrategi formuleret i en “mixed logical dynamical” systemstruktur, som karakteriserer adfærden af den diskretiserede Preisach hysterese i sit udgangssignal. Den tredje strategi inkorporerer den dissiperede energi i kostfunktionen for problemet som en skadesurrogat, hvilket overfører skades- og spredningsegenskaberne fra Preisach hysteresen til Duhem hysteresen; sidstnævnte har den fordel at være beskrevet som en differentialligning.

Endelig foreslåes en strategi til driftsoptimering af vindmølleparker med modstridende objektiver, hvilket tillader operatøren af vindmølleparken at afbalancere elproduktionen og vindmøllernes slid. Dette er af særlig interesse, når man overvejer integration af vindmølleparker i elmarkedet.

Dette arbejde bidrager til den nuværende indsigt indenfor estimering af slitageskader i vindmøllekomponenter, og hvordan man syntetiserer kontrolstrategier, der omfatter hysterese operatorer. Desuden bidrager dette arbejde også til at tage fat på problemet med modstridende objektiver indenfor vind energi konverteringssystemer, nemlig maksimering af effektudvinding og lindring af mekanisk belastning.

1 | Introduction

"Every new beginning comes from some other beginning's end."
~Seneca the Younger

This chapter provides an introduction and the motivation behind this thesis, as well as the basic operating principles and control objectives of wind energy conversion systems. Subsequently, the research challenges and hypotheses underlying this work are presented. Lastly, the contributions of this thesis are outlined.

1.1 Introduction

Electricity has become an essential commodity for modern society's functioning. Power systems have an intrinsic variable nature due to the fluctuations of the load demand, so broadly speaking, electricity production needs to match consumption almost instantaneously to guarantee uninterrupted service to the consumers [Kundur et al., 1994]. Thus, ensuring that this vital commodity supply meets its demand on a real time basis can be quite challenging, due to several reasons such as: 1) the fact that electricity cannot be conveniently stored in large quantities, 2) an ever growing demand caused by population growth, and 3) generation facilities being geographically separated from consumption sites.

Traditionally, balancing production and consumption has been achieved by matching the production to the varying consumption. Nevertheless, fossil fuel depletion, environmental concerns and other political and economical factors have pushed for an increase of renewable energy sources integration in the electricity grid. Wind and solar energy generation systems are examples of such renewable energy sources which are widely available with a relatively low cost, and smaller carbon footprint. The previous has led to an increase in penetration of this type of technologies, which comes as a change of paradigm, namely, change from a centralized generation to a decentralized or distributed generation. This increasing trend in wind energy can be corroborated in Figure 1.1, where the global cumulative installed capacity is shown for recent years. An additional challenge is the variability that energy sources such as the wind exhibit, which often requires compensation. That variability is also affected by political decisions and subsidies, for instance.

Incorporation of renewable energy sources in electrical grids has gained much attention lately, since changes are required in their planning and operation to keep them functioning within specifications [Slootweg & Kling, 2003, Farhangi, 2010, Molderink et al., 2010, Slootweg et al., 2011]. Every unit connected to the grid must follow a stipulated and predefined set of rules imposed by an authority responsible for system integrity and secure operation of the grid. These rules are also known as grid codes and entail much more than a mere balancing of production against consumption, since frequency deviations, power quality, and voltages in cables should be kept within certain bounds [Energinet.dk, 2014, ENTSO-E, 2015]. For power producing units, these grid codes specify the requirements towards the unit in case of faults or disturbances. They also regulate distribution grids, for example, the power quality that has to be maintained such that household equipment works properly.

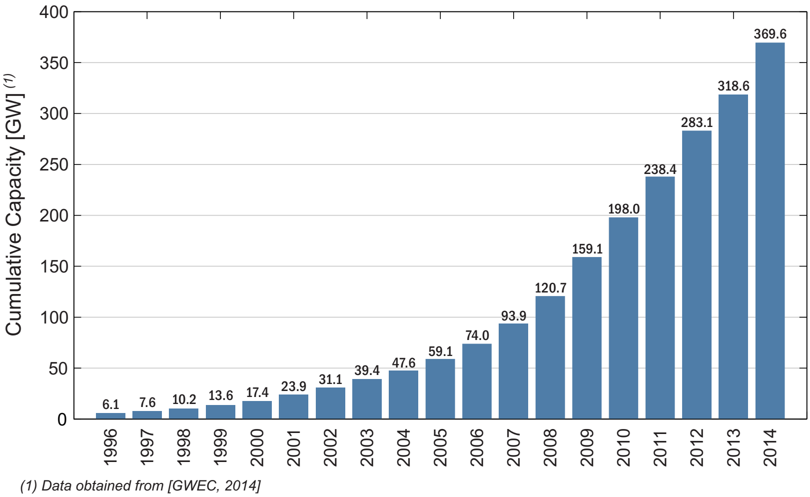

Figure 1.1: Global cumulative wind energy installed capacity from 1996 to 2014 (from [GWEC, 2014]).

Furthermore, the grid is structured in different levels according to its voltage, i.e., high, medium and low voltage. Traditionally, generation is collocated in the high voltage level and then the electricity is transported through medium voltage to households connected in the low voltage level. With the increased popularity of renewables —such as wind turbines, solar panels and combined heat and power units— more distributed generation has been added to grids in medium and low voltage levels, posing new operating challenges.

All the previous challenges have motivated the development of intelligent solutions to revolutionize the electrical grids, which strive to make more flexible, accessible, reliable and economical electrical grids [ESGTP, 2006, Litos, 2008]. These solutions fall under the umbrella term of *smart grid* and are forwarded by advancements in disciplines like electrical engineering, control theory, telecommunications engineering, and economy. For example, in the recent years many solutions for demand response, asset coordination, portfolio optimization, market integration and flexibility management have been proposed, e.g., [Albadi & El-Saadany, 2008, Callaway & Hiskens, 2011, Edlund et al., 2011].

1.2 Wind Energy Conversion Systems

As explained in [Doyle et al., 2013], without control systems there would be no technological development, since control systems are what make machines (or systems) function (or behave) as intended. Such is the case of wind turbines, which very broadly speaking require the assistance of controllers to secure their nominal operation; a regular wind turbine is depicted in Figure 1.2. The primordial task of wind energy systems is to generate electricity, and as such they are designed to minimize the energy generation cost while adhering to power quality standards and safety regulations. This involves a mixture of control objectives [Bianchi et al., 2006], namely:

I. Maximization of energy extraction,

II. Reduction (minimization) of mechanical loads, and

III. Fulfillment of power quality standards.

Figure 1.2: Wind Turbine in North Jutland, Denmark near the E45 highway.

Clearly, there is a trade-off between these goals, particularly (I) and (II), since the wind acts both as prime mover for the energy generation and as the driving fatigue mechanism, specifically the wind turbulence intensity [Riziotis & Voutsinas, 2000]. In the case of (III), the power quality is dictated by the power grid codes to which the turbine is connected.

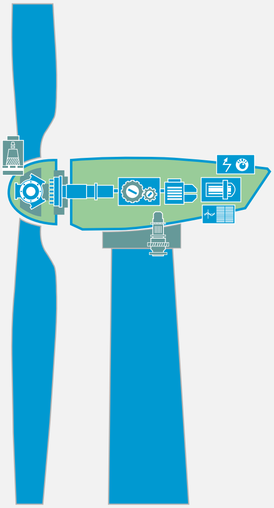

Component	Cost % (continued)	Maintenance Cost %(2)
Rotor blades	24.85%	7.32%
Rotor hub	1.53%	2.69%
Pitch system	2.98%	1.78%
Rotor bearings	1.37%	7.48%
Main shaft	2.14%	0.33%
Gearbox	14.45%	38.11%
Generator	3.85%	8.85%
Power converter	5.61%	2.32%
Brake system	1.48%	0.91%
Yaw system	1.40%	23.15%
Transformer	4.02%	1.28%
Cables + screws	2.24%	5.78%(3)

Component	Cost %(1)
Tower	29.44%
Nacelle housing	1.51%
Main frame	3.13%

(1) Schematic and costs form [Wind Directions, 2007], normalized to add up to 100%. (2) Maintenance costs obtained from [Martin-Tretton, et al., 2011]. (3) Miscellaneous costs.

Figure 1.3: Acquisition and maintenance costs for a 2MW wind turbine.

In Figure 1.3 a schematic of a wind turbine's components is depicted together with acquisition costs and maintenance costs per component, based on [EWEA, 2007]. The cost per component corresponds to the REpower MM92 (2MW) wind turbine and was obtained and normalized from [EWEA, 2007]. The maintenance costs were obtained from [Martin-Tretton et al., 2012] for the 1.5MW-2MW case in 2010. Even though this figure is just for illustrative purposes, on one hand one can see that the most expensive parts of the turbine are the tower, followed by the blades, and then the gearbox-shaft-generator ensemble. On the other hand, from the maintenance side the gearbox and the yaw system are the most problematic, followed by the generator, rotor bearings and blades. The maintenance case is relevant for the work presented in this thesis, where the fatigue-damage in the drive train is considered.

1.3 Benchmark Wind Turbine

The wind turbine plant model considered in this thesis is based on the standard NREL 5MW wind turbine [Jonkman et al., 2009]. We lean on the NREL 5MW wind turbine since it makes comparison with other solutions possible, making it thus a de facto benchmark. [Paper A–C] use a non-linear `Simulink` model based on the standard NREL 5MW turbine. [Paper D] considers a linearized version of the aforementioned non-linear model around a chosen operating point. Lastly, [Paper E–F] rely on the FAST v7 high-fidelity aeroelastic code of the same turbine [Jonkman & Buhl Jr, 2005]. Accordingly, the most relevant aspects of the nominal operation of this turbine are discussed in the sequel. In a smart grid context, wind turbines could contribute to grid balancing by lowering their power output below the rated power, also known as operating in derated mode; however, a financial incentive is necessary for this to make sense.

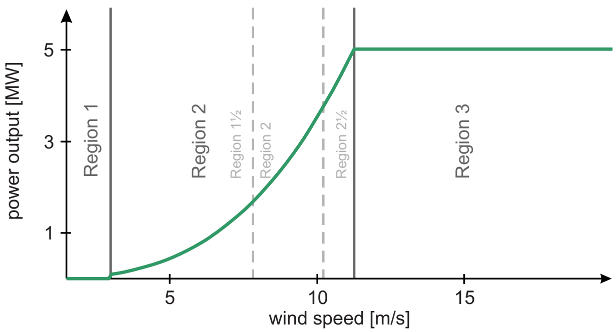

Figure 1.4: Power curve for the NREL 5MW wind turbine divided in three regions. Region 1: Zero power output, Region 2: Maximum power production until nominal power is reached, Region 3: Full-load or nominal power [Jonkman et al., 2009].

The standard generator power output is depicted in Figure 1.4, which is divided in three modes of operation or regions. In Region 1, the wind speed is too low and the power output and generator torque are zero; instead, the wind is used to accelerate the rotor for starting up the turbine. In Region 2, maximum power is produced until nominal power is reached; in this region the generator torque is proportional to the squared generator speed. In Region 3, the power output is capped to the nominal value and kept constant. Sometimes the transition regions 1½ (Region 1 $\rightarrow$ Region 2) and 2½ (Region 2 $\rightarrow$ Region 3) are considered, which are used for a smoother operation transition to the next region. In Figure 1.4 Regions 1, 2, 3 are marked by solid lines and Regions 1½, 2½ are marked by dashed lines. The proposed controllers in this thesis assume an operation under Region 3.

The steady states of other relevant variables with respect to wind speed are also depicted in Figure 1.5 [Jonkman et al., 2009]. It is worth noting that before Region 3 the pitch angle is set to zero; once in Region 3 the pitch angle increases to maintain the power extraction since the generator speed and the generator torque are kept constant such that the power output is maintained at its nominal value.

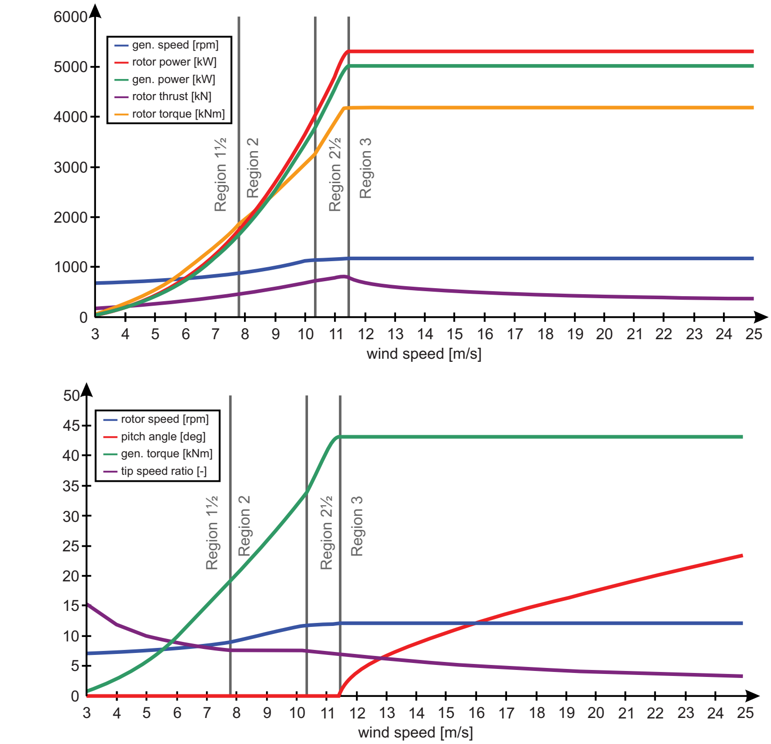

Figure 1.5: Steady state values for the NREL 5MW wind turbine with respect to wind speed [Jonkman et al., 2009].

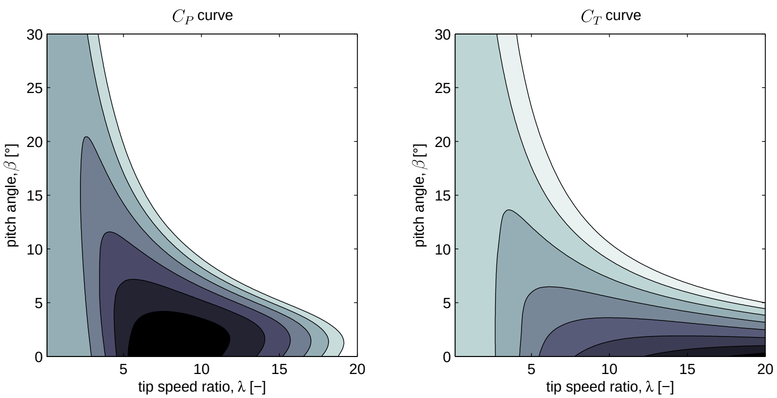

Figure 1.6: Contour plots of the non-dimensional C_P and C_T curves. Notice that only the positive part of the curves is shown.

Two important functions (curves) that characterize the operation of a wind turbine are the non-dimensional thrust and power coefficients, C_T and C_P, respectively. On one hand, the C_P curve dictates the amount of power that can be extracted from the wind; the maximum attainable theoretical value of the C_P curve is $\max\{C_P\} = 16/27 \approx 0.593$ and it is known as the Betz limit —this value is around 0.45 for commercial turbines [Bianchi et al., 2006]. On the other hand, the C_T curve governs the aerodynamic force. Both power C_P and thrust C_T coefficients for the NREL 5MW turbine are shown in Figure 1.6 as functions of the pitch angle and the blade tip speed ratio (a rational function proportional to the rotor speed divided by the wind speed seen at the disc). Generally, C_T and C_P are given as look-up tables; it is worth mentioning that this is done under the assumption that the aerodynamics involved possess quasi-steady properties, i.e., when the wake is in equilibrium with the aerodynamic loads, which does not consider the dynamic inflow effects [Hansen et al., 2006].

1.4 Wind Turbine and Wind Farm Control Overview

Before presenting the overview of wind turbine and wind farm control, the different scales present in such problems are discussed. As introduced earlier, wind turbine and farm operation require the consideration of a mixed control objective, namely power maximization (I) and mechanical load minimization (II). Such trade-off is similar to the ones present in mean-variance portfolio optimization in finance where two competing objectives are considered [Zhou & Li, 2000,Herzog et al., 2007], and sensitivity integrals (waterbed effect) in classical feedback control [Skogestad & Postlethwaite, 2007]. Due to this trade-off, posing the question of fatigue representation for its inclusion in design of control strategies for wind turbines becomes of special interest. Fatigue is a microscopic phenomenon manifesting itself as damage in different levels, ranging from microscopic cracks to damage in components and structures. However, control of wind turbines requires operation on system level which is on the macroscopic scale. Moreover, a wind farm is a collection of several wind turbines with different spatial arrangements affecting the wind flow between them —interacting at the mesoscale level, relevant for meteorological phenomena such as wind.

This difference in spatial scale is sketched in the vertical axis of Figure 1.7, where material, component, turbine and farm levels are depicted. Furthermore, it is also important to consider the time scale involved specially in the wind farm level due to the market integration, whose time scale depends on the market type that is being considered. Power quality could fit in a fast time scale, not being market-driven but enforced by the grid codes. Accordingly, different modeling approaches and problem formulations are needed depending on which aspect one would like to focus on, namely: fatigue in crack level, fatigue in component level, individual wind turbine control, aerodynamic coupling between turbines, wind farm market integration, etc. It is also interesting to observe the wind or van der Hoven spectrum [van der Hoven, 1957, Bianchi et al., 2006], hinting at the multi-time scale discussed before, which is shown at the bottom of Figure 1.7. Lastly, this figure also shows in dark red calligraphic font the relationship between these topics and the contributions of this thesis.

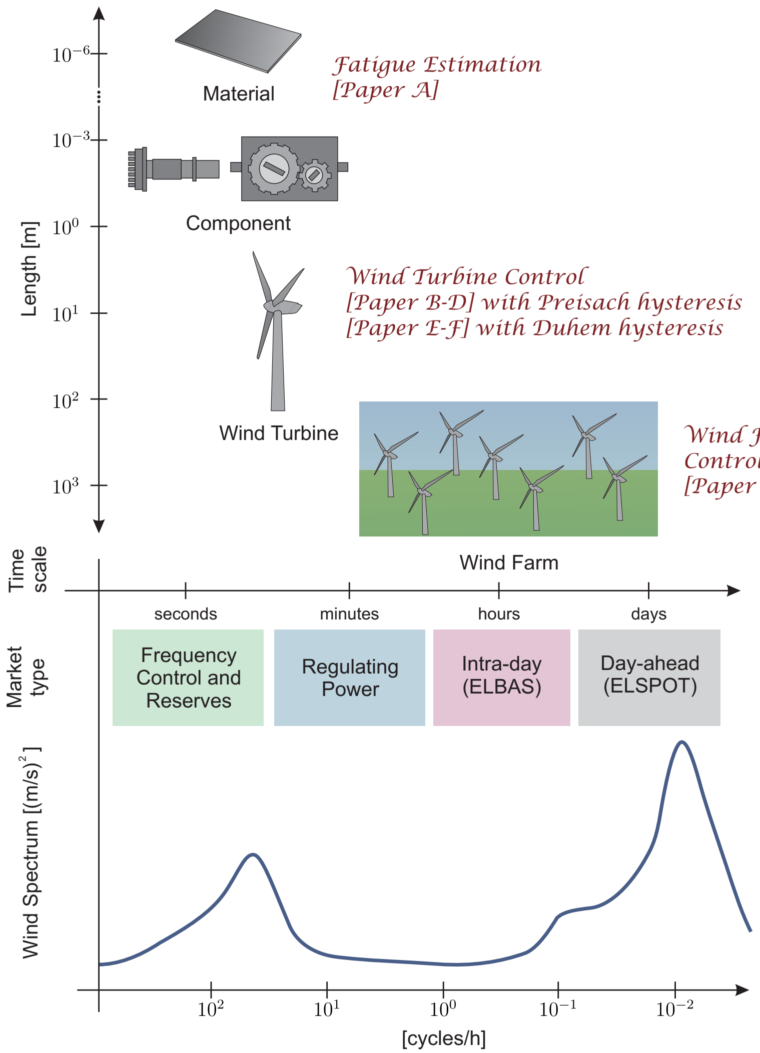

Figure 1.7: Sketch of spatial and temporal scales, relating the relevant topics to the contributions of this thesis. Additionally, different electricity markets and the wind spectrum are shown.

The ultimate purpose of wind energy conversion systems is extracting power from the wind and delivering it to the power grid. The previous entails an interface between mechanical and electrical power. In this thesis the focus is on the mechanical side. Control of wind turbines from the electrical power counterpart can be achieved through power electronics [Chen et al., 2009, Blaabjerg et al., 2012]. In broad terms for the mechanical part, the controllers present in a wind turbine are the generator torque, pitch angle and yaw angle controllers. The yaw controller changes the nacelle point to the wind and is slower than the torque and pitch controllers [Johnson et al., 2006]. Therefore, the existing wind turbine control methodologies can be categorized in very broad terms as:

- **Classical Control strategies.** The classical strategies address the generator torque and the pitch angle control. For the torque control the typical strategy follows the behavior of the torque shown in Figure 1.5 being zero for Region 1, increasing for Region 2 and being constant in Region 3; in Region 2 the controller consists of a gain times the generator speed squared (thus also known as omega-squared control) [Bossanyi, 2000, Bossanyi, 2003, Pao & Johnson, 2009]. In Region 3 where the torque is kept constant to maintain the rated power, the pitch controller takes over generally being scheduled PI controllers. The baseline controller for the NREL 5MW turbine also falls under this category, since the generator torque is computed as a tabulated function of the generator speed depending on the operating region, and the pitch angle controller is a PI [Jonkman et al., 2009]. Improvements include damping resonances and controlling pitch angle individually [Bossanyi, 2003, Bossanyi, 2005, Larsen et al., 2005].

- **Optimization-based and Advanced Control Strategies.** Advanced and modern control strategies for wind turbines have been extensively addressed in the literature, perhaps due to the optimality guarantees granted by optimal control, to the advent of mathematical optimization caused by the increase in computational resources, and to the maturity of the wind turbine industry itself. Accordingly, wind turbine control strategies have been proposed using optimal control [Hammerum et al., 2007, Munteanu et al., 2008] and model predictive control [Soltani et al., 2011, Friis et al., 2011, Adegas et al., 2013, Mirzaei et al., 2013]. Other advanced control strategies include control of linear parameter varying systems [Bianchi et al., 2006, Adegas et al., 2012], and robust/fault-tolerant control [Sloth et al., 2011, Odgaard et al., 2013].

- **Wake-oriented Control Strategies.** Another way of formulating the control problem is to address the wakes or wind flows interacting with the wind turbine. This also gives a natural connection between wind turbines for the wind farm level. As discussed in [Annoni et al., 2015], there are different ways to characterize such interaction (also with different complexity) ranging from engineering to computation fluid dynamics models, e.g., [Schepers & Van der Pijl, 2007, Soleimanzadeh & Wisniewski, 2011, Johnson & Fritsch, 2012, Gebraad et al., 2014, Fleming et al., 2014].

The references in the previous classification are not meant to be exhaustive and they just constitute a subset of the numerous control methodologies in the literature.

For the wind farm case, an alternative classification is to categorize control strategies as: power maximization, power reference tracking and individual turbine load minimization; further details can be found in [Knudsen et al., 2014], and the references therein. This classification largely reflects the control objectives of wind energy conversion systems described in (I)-(III).

1.5 Research Challenges and Hypotheses

From the previous discussions it is clear that wind energy systems will be key in the development of the smart grid concept and will help in conquering some of the challenges that come with the smart grid. Incorporation of such electricity generation sources poses challenges in terms of lifetime guarantees, operation, reliability, energy balancing and market integration, among others. Specifically, wind turbines could help damp transient behavior due to their fast dynamics. However, they also introduce a variability that needs to be compensated. Addressing the mixed-objective of power maximization and mechanical load reduction contributes to solve some of the aforementioned challenges and therefore, fatigue estimation takes a central role in this thesis. The source of this trade-off lies in the fact that the wind is both the energy generation driver and the main fatigue propagation mechanism. This observation is useful to incorporate fatigue-damage into optimal control problem formulations, where lifetime degradation can be penalized.
The above discussion leads to the following hypotheses:

1. Damage caused by fatigue in the component scale can be quantified by means of an operator or mathematical function which can be formulated in closed mathematical form.

2. This operator or mathematical function has a physical interpretation and can be included in optimal control problems.

3. Reducing fatigue-damage in a component will extend its operational lifetime.

4. Material energy dissipation is proportional to damage.

The following assumptions are made on this thesis:

1. Rainflow counting is the standard for fatigue-damage characterization. The material specific parameters corresponding to component can be obtained from an S-N curve and used to scale the damage, which accumulates linearly.

2. For controller design in the wind turbine level, the wind turbine non-linear behavior is well approximated by a linearized model around certain operating point.

3. In the wind farm level, power is well captured by the mean value and mechanical loads are captured by the mean and the turbulence intensity.

1.6 Outline of the Thesis

This thesis is divided in two parts. The first part is a comprehensive introduction, containing the background, motivation, preliminaries, extended summary of the contributions and closing remarks. The second part is comprised of the publications enclosed as [Paper A–G], presenting the contributions in detail. The contributions are described as follows:

Paper A [Barradas-Berglind & Wisniewski, 2015b]

The aim of this paper is to address the applicability of the most recognized fatigue-damage estimation methods to control of wind turbines. Therefore, in this paper the most recognized approaches to estimate the damage caused by fatigue in the component level are categorized, discussed and compared. The focus of this paper is on representation of fatigue-damage and it serves as a starting point for this thesis.

Paper B [Barradas-Berglind et al., 2015c]

By means of the Preisach hysteresis operator fatigue-damage estimation technique discussed in [Paper A] that characterizes damage in the rainflow counting sense, this paper proposes a modified damage-reduction model predictive control strategy for wind turbines. The main purpose is to include a model of the fatigue-damage of the wind turbine components in the controller design and synthesis process. Hence, the proposed strategy incorporates an online fatigue estimation method through the objective function, where the ultimate goal in mind is to reduce the fatigue-damage of the drive-train. The outcome is an adaptive or self-tuning predictive control strategy for wind turbine fatigue-damage reduction, which relies on parameter identification of previous measurement data. DOI: `http://dx.doi.org/10.1049/iet-cta.2014.0730`

Paper C [Barradas-Berglind et al., 2015d]

Parting from the results in [Paper B], the damage reduction predictive control strategy is extended to consider state, input, and slew rate constraints. As in [Paper B] the online damage estimation is incorporated through the weighting matrices, resulting in a convex problem. Lastly, the damage provided by the hysteresis variations is compared against the estimated one. DOI: `http://dx.doi.org/10.1109/ACC.2015.7171908`

Paper D [Barradas-Berglind & Wisniewski, 2015a]

In this paper linear time invariant systems with discretized Preisach hysteresis output are incorporated into the mixed logical dynamical systems framework, such that the Preisach hysteresis can be included in control settings. Consequently, instead of the recursive estimation proposed in [Paper B–C], the estimated damage given by a discretized Preisach operator can be directly included in the cost functional of the optimization problem. The results of this strategy are evaluated for three different cases and the impact in the control effort is analyzed.

Paper E [Barradas-Berglind et al., 2015b]

In this paper an active damage reduction control strategy for wind turbines based on hysteresis operators dissipated energy is proposed, relying on the equivalences relating both damage in the rainflow counting sense and dissipated energy to the variations of Preisach hysteresis operators. In contrast to [Paper B–D], the Duhem hysteresis model is adopted instead of the Preisach hysteresis model, since it has the amenity of being described by a differential equation. Accordingly, the dissipated energy of the Duhem model is incorporated into the optimal control problem formulation as a surrogate or proxy to the damage in the drive-train.

Paper F [Barradas-Berglind et al., 2015a]
Parting from the results in [Paper E], the dissipation properties of the Preisach hysteresis operator are studied. Consequently, it is shown that the dissipation of a Preisach hysteresis operator is equivalent to the total variations of a scaled Preisach hysteresis operator.

Paper G [Barradas-Berglind & Wisniewski, 2015c]
In contrast to [Paper B–F], this work is centered on the wind farm level. Hence, the focus is on addressing and solving the mixed-objective optimization problem for the operation of a wind farm, which considers both power maximization and mechanical load minimization. The intention is to provide a strategy that allows to operate a wind farm in different ways, depending on whether maximizing power production or reducing turbines wear is more relevant. This becomes of special interest in smart grid settings where electricity markets push to consider not only the power production but also the lifetime degradation of the infrastructure.

2 Fatigue-Damage and Hysteresis

> *"Tempus edax rerum (Time, devourer of all things)"*
>
> *~Ovid*
>
> *This chapter gives a background on fatigue-damage and the rainflow counting algorithm for damage estimation. It also serves as a prevue to [Paper A] where the most recognized fatigue-damage estimation methods are discussed. Subsequently, hysteresis operators together with their properties are described, which are employed in [Paper B–F]. Lastly, the equivalence between symmetric rainflow counting and the variations of a Preisach hysteresis operator is presented.*

Fatigue is a critical factor in structures and materials exposed to harsh operating conditions, both in the design stage and during the control of their operation. It is regarded as a critical factor in structures such as wind turbines, where it is necessary to ensure a certain life span under both normal and transient operating conditions — such as start-up and shut-down— in a turbulent environment. In general, fatigue can be understood as the weakening or breakdown of a material subject to stress, especially cyclic stresses. Damage is caused by loading on a material structure resulting in deformations or cracks, compromising its integrity as a result. Accordingly, fatigue is a phenomenon that occurs in a microscopic scale, manifesting itself as deterioration or damage. Fatigue has been extensively studied, and the literature is vast and approached from diverse points of view.

2.1 Rainflow counting

Rainflow counting is perhaps the most recognized measure of fatigue and tool for lifetime assessment. Its name comes from the analogy made of roofs collecting water, also giving rise to the more peculiar name of pagoda roof. There are different algorithms such as the original one from [Endo et al., 1967] and more recent improvements [Downing & Socie, 1982, Rychlik, 1987], but they all rely on a counting procedure that extrapolates information from extrema, i.e., maxima and minima, of a time series. Subsequently, this count is weighted and added using the Palmgren-Miner rule [Palmgren, 1924, Miner, 1945] for damage accumulation. A sketch of the rainflow counting algorithm is presented in Figure 2.1.

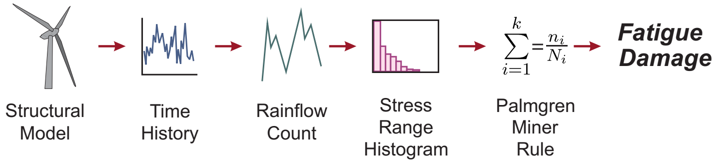

Figure 2.1: Rainflow counting damage estimation procedure.

For many materials there is an explicit relation between number of cycles to failure and cycle amplitude, known as S-N or Wöhler curves, given as a line in a log-log scale as

$$s^m N = K, \tag{2.1}$$

where m and K are material specific parameters —also known as S-N coefficients— and N is the number of cycles to failure at a given stress amplitude s. A sample S-N curve is shown in Figure 2.2. Then, for a time history, the total damage under the linear accumulation damage rule due to Palmgren and Miner is given as

$$D(T) = \sum_{i=1}^{N(T)} \Delta D_i = \sum_{i=1}^{N(T)} \frac{1}{N_i}, \tag{2.2}$$

for damage increments ΔD_i associated to each counted cycle, N_i the number of cycles to failure associated to stress amplitude s_i, and the number of all counted cycles $N(T)$. Taking the S-N curve relationship in (2.1), we can rewrite (2.2) as

$$D(T) = \frac{1}{K} \sum_{i=1}^{N(T)} (s_i)^m. \tag{2.3}$$

Notice that the rainflow count algorithm provides the cycles to failure associated to amplitude s_i.

In the left side of Figure 2.3 an example of a rainflow counting algorithm is presented. Following the explanation in [Radaj & Vormwald, 1995, Krupp, 2007], the starting "rain" flows off all strain amplitudes as if they were roofs. Then the flow ends when: i) the rain water flow meets rain water from a higher roof (e.g., E-G ends in F or C-E ends in D); ii) the flow reaches a load value where the opposite load minimum falls below the starting minimum (e.g., 0-A-F-G with respect to H); iii) the flow reaches a load value where the opposite load maximum is higher than the starting maximum (e.g., A-B-D-E with respect to G); iv) there is no further roof to continue (e.g., L and T).

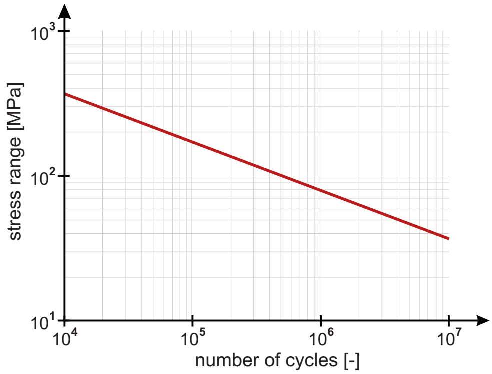

Figure 2.2: S-N material curve example. Notice both axis are in logarithmic scale.

Each rain water flow from start to end is considered as half a cycle. Half cycles of the same size, but with opposite direction result in a full cycle. Lastly, the rain flows ending in arrows at the lower part of the diagram correspond to leftover half loops.

The rainflow counting algorithm essentially identifies the ranges of strain which correspond to closed hysteresis loops [Downing & Socie, 1982]; hence, the algorithm only counts a hysteresis loop when it is completed. This is also exemplified on the right side of Figure 2.3, where open and closed hysteresis loops are shown in the stress-strain plane. The phenomenon of hysteresis will be addressed in the following.

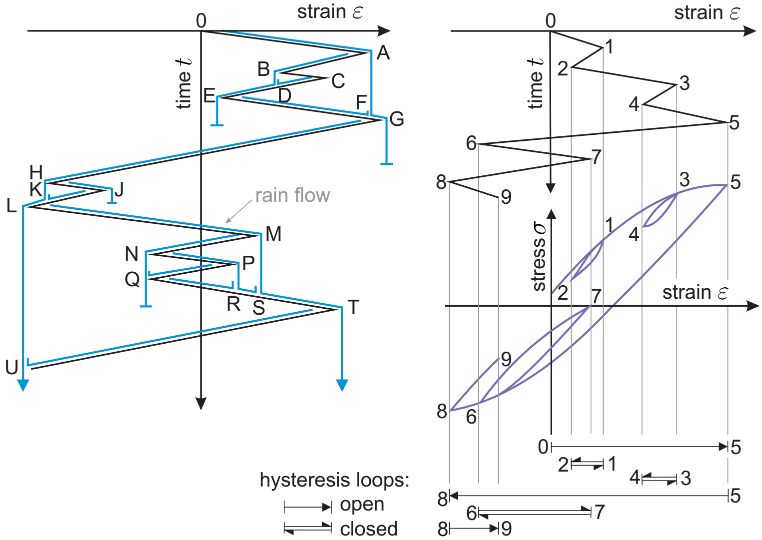

Figure 2.3: Rainflow counting algorithm and its relation to hysteresis loops (after [Radaj & Vormwald, 1995, Krupp, 2007]).

Other areas where rainflow counting is used include oceanography [Brodtkorb et al., 2000], damage caused by road irregularities [Bogsjö & Rychlik, 2009], and battery lifetime estimation [Swierczynski et al., 2011]

2.2 Hysteresis

Hysteresis is a strongly non-linear complex phenomenon characterizing the relation between two scalar time dependent quantities that cannot be expressed in terms of a single valued function, but such relationship takes the form of loops as in Figure 2.4 [Brokate & Sprekels, 1996]. In this figure the input-output behavior of hysteresis is exemplified, where v and w can take different physical meanings, like stress versus strain, electric displacement versus electric field, or magnetic field versus magnetization. Hysteresis appears across different disciplines such as mechanics [Dahl, 1976, De Wit et al., 1995], ferromagnetics [Jiles & Atherton, 1986, Coleman & Hodgdon, 1987], seismology [Sucuoğlu & Erberik, 2004], engineering [Jayawardhana et al., 2008], economy [Franz, 1990] and biology [Tyson & Novak, 2001]. Moreover, it can be purposely added such as systems with thermostats [Malhame & Chong, 1985] or switching [Wisniewski & Leth, 2011].

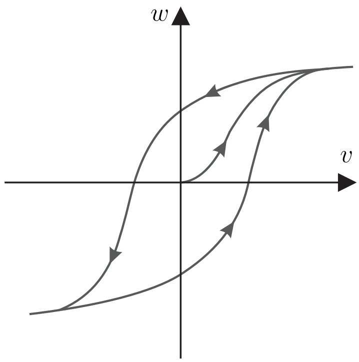

Figure 2.4: Typical hysteresis behavior for two quantities v and w.

The most typical type of hysteresis occurs for the rate independent case, which implies that only the loops themselves are important, not how fast they are traversed. Rate independent processes are mathematically formalized as hysteresis operators [Krasnosel'skiĭ & Pokrovskiĭ, 1989, Mayergoyz, 1991, Brokate & Sprekels, 1996].

2.3 Hysteresis Operators

The definition of hysteresis operators presented below is based on the framework of [Brokate & Sprekels, 1996]. This section is instrumental for the further understanding of the Preisach and Duhem hysteresis operators. Consider the operator equation relating an input function v to an output function w,

$$w(t) = \mathcal{W}[v](t), \quad \text{for } t \in [t_0, t_f]. \tag{2.4}$$

for a functional $\mathcal{W}$.

Definition 1. *Let I be a nonempty interval of $\mathbb{R}$. We call a function $v : I \to \mathbb{R}$*

- *increasing (strictly increasing) on I, if $v(\tau) \leq v(t)$ (resp., $v(\tau) < v(t)$) whenever $\tau, t \in I$ and $\tau < t$.*
- *monotone (strictly monotone) on I, if either v or $-v$ is increasing (strictly increasing) on I.*

Furthermore, a continuous function $v : [t_0, t_f] \to \mathbb{R}$ is called piecewise monotone if there exists a sequence $\{t_i\}_{0<i<n}$ such that $0 = t_0 < t_1 < \ldots < t_{N-1} < t_N = t_f$ and v is monotone on all subintervals $[t_i, t_{i+1}]$.

Denote the set of continuous piecewise monotone functions on $[t_0, t_f]$ by $C_{pm}[t_0, t_f]$.

Definition 2 (Rate independence). [Brokate & Sprekels, 1996] *Let a time transformation $\phi : [t_0, t_f] \to [t_0, t_f]$ be an increasing continuous function satisfying $\phi(t_0) = t_0$ and $\phi(t_f) = t_f$. A functional $\mathcal{W} : C_{pm}[t_0, t_f] \to C_{pm}[t_0, t_f]$ is rate independent if and only if*

$$\mathcal{W}[v \circ \phi](t) = \mathcal{W}[v] \circ \phi(t), \tag{2.5}$$

for any $v \in C_{pm}[t_0, t_f]$ and any ϕ on $[t_0, t_f]$, where $\circ$ denotes functional composition.

Definition 3 (Volterra property). [Brokate & Sprekels, 1996] *We say that an operator $\mathcal{W} : C_{pm}[t_0, t_f] \to C_{pm}[t_0, t_f]$ has the Volterra property whenever v_1, $v_2 \in C_{pm}[t_0, t_f]$ and $t \in [t_0, t_f]$ we have $v_1(t) = v_2(t)$ implies $\mathcal{W}[v_1](t) = \mathcal{W}[v_2](t)$.*

Definition 4 (Hysteresis operator). [Brokate & Sprekels, 1996] *An operator $\mathcal{W} : C_{pm}[t_0, t_f] \to C_{pm}[t_0, t_f]$ is called a hysteresis operator if it is rate independent and has the Volterra property.*

2.4 Preisach Hysteresis

Let $s = (v_0, \cdots, v_n) \in S$ be a given string and S be the space of finite sequences in $\mathbb{R}$, i.e., $S = \{(v_0, v_1, \cdots, v_n) : n \in \mathbb{N}_0, v_i \in \mathbb{R}, 0 \leq i \leq n\}$.

Definition 5 (Relay hysteresis operator). *Let $\beta, \alpha \in \mathbb{R}$ with $\beta < \alpha$ and $w_{-1} \in \{0, 1\}$ be given. We define the relay hysteresis operator $\mathcal{R}_{\beta,\alpha} : S \to S$ by*

$$\mathcal{R}_{\beta,\alpha}(v_0, \cdots, v_n) = (w_0, \cdots, w_n), \tag{2.6}$$

$$\textit{with} \qquad w_i = \begin{cases} 1, & v_i \geq \alpha, \\ 0, & v_i \leq \beta, \\ w_{i-1}, & \beta < v_i < \alpha. \end{cases} \tag{2.7}$$

Definition 6 (Preisach hysteresis operator). *Let $M \in \mathbb{R}$ be an a priori bound for admissible input values, then define the Preisach plane as*

$$P = \left\{(\beta, \alpha) \in \mathbb{R}^2, -M \leq \beta \leq \alpha \leq M\right\}. \tag{2.8}$$

Let the density function $\rho(\alpha, \beta)$ with compact support in P be given, i.e., equal to zero outside the triangle P. We define the Preisach hysteresis operator $\mathcal{W} : S \to S$ as

$$\mathcal{W}(s) = \int_{\beta<\alpha} \rho(\alpha, \beta)\mathcal{R}_{\beta,\alpha}(s)d\beta d\alpha. \tag{2.9}$$

Here, the integral is understood to be component-wise with respect to the elements of the string $\mathcal{R}_{\beta,\alpha}(s)$. Consequently, the relevant threshold values for the relays $\mathcal{R}_{\beta,\alpha}$ will lie within the triangle P. Notice that the Preisach operator in (2.9) is a hysteresis operator according to Definition 4 since it is rate independent and has the Volterra property.

2.5 Connection to Damage via Variations

Let a string $s = (v_0, \cdots, v_n)$ represent an arbitrary load sequence. Following the interpretation of rainflow counting given in [Brokate & Sprekels, 1996], one can introduce $\mathcal{N}(\beta, \alpha)$ with values β and α, chosen such that the input string s with $v_{2k} = \beta$ and $v_{2k+1} = \alpha$ for $k \in \mathbb{N}_0$ destroys the specimen after $\mathcal{N}(\beta, \alpha) = \tilde{\mathcal{N}}(|\alpha - \beta|)$ cycles. The resulting curve is an S-N or Wöhler curve since the ansatz

$$\tilde{\mathcal{N}}(\beta, \alpha) = \kappa_1 |\beta - \alpha|^{\kappa_2} \tag{2.10}$$

exhibits a straight line in a log-log scale, where κ_1 and κ_2 are scaling constants and $|\beta - \alpha|$ is a given stress range; this relationship actually corresponds to (2.1) with $\kappa_1 = 1/K$ and $\kappa_2 = m$.

Subsequently, the Palmgren-Miner rule is used to identify and count cycles for an arbitrary load sequence $s \in S$, such that the damage accumulation is obtained as

$$D_{ac}(s) := \sum_{\beta<\alpha} \frac{c_{per}(s)(\beta, \alpha)}{\mathcal{N}(\beta, \alpha)}, \tag{2.11}$$

where $c_{per}(s)(\beta, \alpha)$ is the rainflow count associated with a fixed string s, counting between the values of β and α; the damage accumulation in (2.11) corresponds to (2.3).
Define the variation operator *Var* that characterizes the total variations of a signal as

Definition 7 (Variation). *For any string $s = (v_0, \cdots, v_n) \in S$, we define its variation* $\mathrm{Var} : s \to \mathbb{R}$ *by*

$$\mathrm{Var}(s) = \sum_{i=0}^{N-1} |v_{i+1} - v_i|. \tag{2.12}$$

The equivalence provided in [Brokate et al., 1996] and [Brokate & Sprekels, 1996] between symmetric rainflow counting and a Preisach hysteresis operator, is given as follows

Proposition 1 (Damage equivalence). [Brokate & Sprekels, 1996] *Let $\mathcal{W}^{per}(s)$ be the periodic version of the Preisach operator such that for each sequence of stresses $s = (v_0, \cdots, v_n) \in S$ with $\|s\|_\infty \leq M$ and $v_0 = v_n$ the total damage $D_{ac}(s)$ associated to s satisfies*

$$D_{ac}(s) = \sum_{\beta<\alpha} \frac{c_{per}(s)(\beta, \alpha)}{\mathcal{N}(\beta, \alpha)} = \mathrm{Var}(\mathcal{W}^{per}(s)), \tag{2.13}$$

where the density function of the Preisach hysteresis $\mathcal{W}^{per}$ is given as

$$\rho(\beta, \alpha) = -\frac{1}{2} \frac{\partial}{\partial \beta} \frac{\partial}{\partial \alpha} \left(\frac{1}{\mathcal{N}(\beta, \alpha)} \right), \tag{2.14}$$

with $\mathcal{N}(\beta, \alpha)$ representing the total number of cycles to failure.

The interpretation of the equivalence in (2.13) is that the rainflow counting algorithm counts the number of oscillations at each range of amplitude, and this is precisely what $\mathrm{Var}\big(\mathcal{W}^{per}(s)\big)$ computes, namely the number of oscillations of the input s between the thresholds β and α. The density function $\rho(\alpha, \beta)$ in (2.14) can also be interpreted as a gain that changes with the different values of β and α, and being a function of $\mathcal{N}(\beta, \alpha)$ which denotes the number of cycles to failure.

It is worth mentioning that the results in Proposition 1 apply to symmetric RFC. As mentioned in [Brokate et al., 1996] not all RFC methods are symmetric. For symmetric RFC the so-called Madelung rules apply, i.e., deletion pairs commute, meaning that the order in which the sequences are deleted does not matter, which is not always the case. By means of the damage equivalence to rainflow counting in Proposition 1 one can incorporate fatigue-damage or wear in components in a control problem, since the Preisach operator has closed mathematical form and acts on measurements (even though it exhibits memory effects). This equivalence under the string framework is used in [Paper A–D], where discretized time signals were used and thus each sample was considered as a string entry.

Remark 1*: Even though the original proposition acts on periodic operators such that the residual of the counting can be included, this is a difficult requirement to fulfill. Hence, the normal Preisach operator is used instead of its periodic version, essentially neglecting the contribution of the rainflow residual. Further details on periodic operators can be found on [Brokate & Sprekels, 1996] and [Paper B].*

3 Hysteresis Operators and Dissipation

"Life can only be understood backwards, but it must be lived forwards."
~Søren Kierkegaard

This chapter introduces the notion of dissipativity for the Preisach hysteresis, where the stored and lost energy are characterized. Consequently, the dissipated energy in the Preisach model is related to the variations of a scaled Preisach hysteresis operator. Subsequently, the dissipation properties of the Duhem hysteresis model are presented. These concepts are key for [Paper E–F].

Previously, the equivalence between damage in the rainflow counting sense and the total variations of certain Preisach hysteresis operator was discussed. In this chapter the dissipation properties of the Preisach and Duhem hysteresis operators are presented. Subsequently, the equivalence between the Preisach hysteresis energy dissipation and its total variations is shown. This agrees with the discussion in [Brokate et al., 1996], where both damage and dissipation are related to variations, boiling down to a difference in Preisach density functions. Accordingly, this scaling factor is determined and shown in Proposition 2.

3.1 Preliminaries

For two open sets $X \subset \mathbb{R}^n$ and $Y \subset \mathbb{R}^m$ we denote $\mathcal{C}^1(X, Y)$ as the space of continuously differentiable functions $f : X \to Y$; if $Y = \mathbb{R}$ we use the notation $\mathcal{C}^1(X) := \mathcal{C}^1(X, \mathbb{R})$. Additionally, we denote $AC(X)$ as the space of absolutely continuous functions $f : X \to \mathbb{R}$. We call a continuous function $u : \mathbb{R}_+ \to \mathbb{R}$ piecewise monotone if there exists a sequence $\{t_i\}_{i\in\mathbb{N}}$ such that $t_0 = 0, t_i < t_{i+1}, \lim_n t_n \to \infty$ and the input u is monotone on each time interval $[t_i, t_{i+1}]$. As previously introduced, the set of continuous piecewise monotone functions on $\mathbb{R}_+$ are denoted by $C_{pm}(\mathbb{R}_+)$.

For every absolutely continuous function $u : \mathbb{R}_+ \to \mathbb{R}$, the total variation $|u|_{[0,\eta]}$

for any $\eta \geq 0$ is given by

$$|u|_{[0,\eta]} := |u(0)| + \int_0^\eta |\dot{u}(t)|\, dt. \tag{3.1}$$

It is easy to show that for every $u \in C_{pm}(\mathbb{R}_+)$, we have that

$$|u|_{[0,\eta]} = |u(0)| + \left(\sum_{i=0}^{N-1} |u(t_{i+1}) - u(t_i)| \right) + |u(\eta) - u(t_N)|\,, \tag{3.2}$$

where the sequence $\{t_i\}_{i\in\mathbb{N}}$ is the one that defines piecewise monotonicity of u. The definition of total variation on $C_{pm}(\mathbb{R}_+)$ in (3.2) above is equivalent to the variation operator *Var* in (2.12), where the string s is represented by the sequence $\{u(t_i)\}_{i\in\mathbb{N}}$.

Remark 2*: A redefinition of the relay hysteresis acting on* u *instead of* s *as in Definition 5 is required, but it will be omitted here since its operating principle is essentially the same. Such definition is given in [Paper F] and follows the one in [Logemann & Ryan, 2003]. In the sequel the outputs of the relay are considered in* $\{-1, +1\}$.

3.2 Energy Exchange in the Preisach Hysteresis

In this section the energy exchange, namely the stored and dissipated energy in the Preisach hysteresis model is described. In order to do this, by fixing the input u one can consider that the relays comprising the Preisach hysteresis are divided in two time-varying sets represented by the regions

$$P_+(t) := \{(\alpha, \beta) \in P \,|\, \big(\mathcal{R}_{\beta,\alpha}(u)\big)(t) = +1\}, \tag{3.3a}$$

$$P_-(t) := \{(\alpha, \beta) \in P \,|\, \big(\mathcal{R}_{\beta,\alpha}(u)\big)(t) = -1\}, \tag{3.3b}$$

such that their union gives the Preisach plane in (2.8), i.e., $P = P_+(t) \cup P_-(t)$. Furthermore, consider the sub-regions of the Preisach plane P defined as

$$\mathcal{Q}_1 = \{(\alpha, \beta) \in P \,|\alpha > 0, \beta > 0\}, \tag{3.4a}$$

$$\mathcal{Q}_2 = \{(\alpha, \beta) \in P \,|\alpha \geq 0, \beta \leq 0\}, \tag{3.4b}$$

$$\mathcal{Q}_3 = \{(\alpha, \beta) \in P \,|\alpha < 0, \beta < 0\}. \tag{3.4c}$$

The Preisach plane P and its sub-regions $\mathcal{Q}_1$, $\mathcal{Q}_2$, $\mathcal{Q}_3$ are depicted in Figure 3.1.

Since the Preisach hysteresis model is basically a superposition of weighted relays, it is useful to start looking at individual properties of those weighted relays. Following [Gorbet, 1998], for a single relay the energy lost in one cycle is equal to $2\rho(\alpha, \beta) \cdot (\alpha - \beta) = q_\alpha + q_\beta$, defined as $q_\alpha := 2\rho(\alpha, \beta)\alpha$ and $q_\beta := -2\rho(\alpha, \beta)\beta$. Hence, the dissipated energy in one cycle for a single relay is the area of the relay, i.e., $q_\alpha + q_\beta$. The previous is depicted in Fig. 3.2 for a given input $u(t)$.

In the approach taken in [Gorbet, 1998], when either q_α or q_β is negative for a given relay, it implies that the energy is recovered from the relay when it switches. This differs from the approach taken in [Mayergoyz, 1991], where it is assumed that

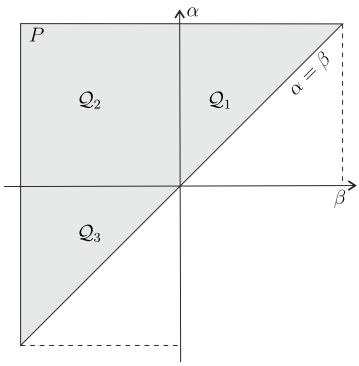

Figure 3.1: Preisach plane P and its sub-regions $\mathcal{Q}_1$, $\mathcal{Q}_2$, $\mathcal{Q}_3$.

Sub-region of P	Switch in relays	Stored energy (Gorbet)	Lost energy (Gorbet)	Lost energy (Mayergoyz)
$\mathcal{Q}_1$	$+1 \to -1$	$\lvert q_\beta \rvert$	0	$\lvert q_\alpha + q_\beta \rvert / 2$
$\mathcal{Q}_1$	$-1 \to +1$	0	$\lvert q_\alpha + q_\beta \rvert$	$\lvert q_\alpha + q_\beta \rvert / 2$
$\mathcal{Q}_2$	$+1 \to -1$	0	$\lvert q_\beta \rvert$	$\lvert q_\alpha + q_\beta \rvert / 2$
$\mathcal{Q}_2$	$-1 \to -1$	0	$\lvert q_\alpha \rvert$	$\lvert q_\alpha + q_\beta \rvert / 2$
$\mathcal{Q}_3$	$+1 \to +1$	0	$\lvert q_\alpha + q_\beta \rvert$	$\lvert q_\alpha + q_\beta \rvert / 2$
$\mathcal{Q}_3$	$-1 \to -1$	$\lvert q_\alpha \rvert$	0	$\lvert q_\alpha + q_\beta \rvert / 2$

Table 3.1: Relays energy transfer for the Preisach model.

the energy loss is split evenly between switches, such that $q_\alpha = q_\beta$. Similar to [Gorbet, 1998], the energy storage capabilities of individual relays are summarized in Table 3.1.

In [Gorbet, 1998, Gorbet et al., 2001] the stored energy for the Preisach hysteresis model is given by

$$\iint_{\mathcal{Q}_1 \cap P_+} |q_\beta| \, d\alpha d\beta + \iint_{\mathcal{Q}_3 \cap P_-} |q_\alpha| \, d\alpha d\beta, \tag{3.5}$$

which corresponds to the behavior presented in Table 3.1. Note that Table 3.1 presents two cases of lost (or dissipated) energy. The first case corresponds to the counterpart of the stored energy in (3.5) as described in [Gorbet, 1998]. The second one corresponds to the approach taken by [Mayergoyz, 1991], where it was assumed that the total energy loss was split evenly between switches, as previously explained for a single relay.

Looking at Table 3.1, one can see the correspondence to the stored energy in (3.5), since it is the recoverable energy. However, if one is interested in the lost or dissipated

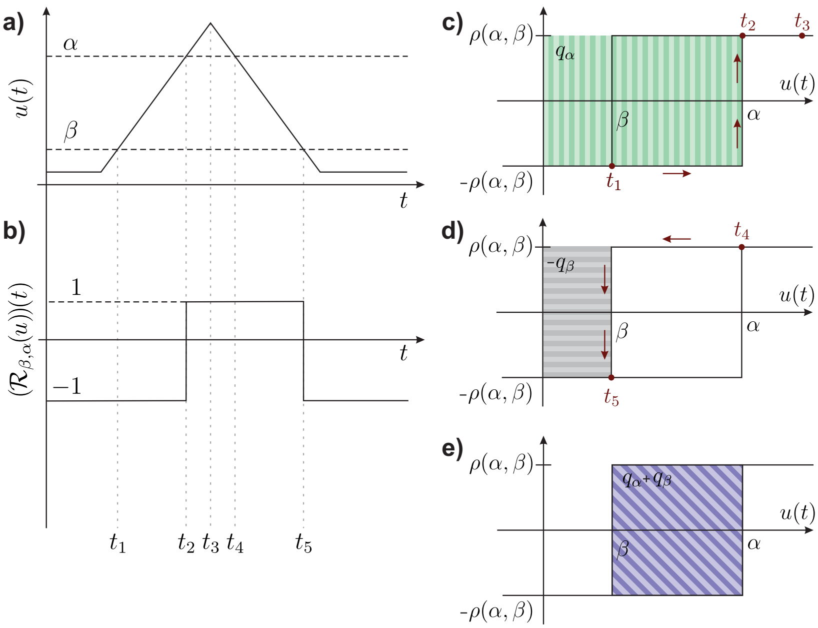

Figure 3.2: Relay energy transfer for one cycle: a) input signal, b) relay output, c) used energy at t_3 (q_α), d) recovered energy at t_5 ($-q_\beta$), e) lost or dissipated energy in one cycle ($q_\alpha + q_\beta$).

energy, then it should be calculated as the complement of the recoverable energy, i.e.,

$$\iint_{\mathcal{Q}_1 \cap P_-} |q_\alpha + q_\beta| \, d\alpha d\beta + \iint_{\mathcal{Q}_3 \cap P_+} |q_\alpha + q_\beta| \, d\alpha d\beta + \iint_{\mathcal{Q}_2 \cap P_+} |q_\beta| \, d\alpha d\beta + \iint_{\mathcal{Q}_2 \cap P_-} |q_\alpha| \, d\alpha d\beta. \tag{3.6}$$

Alternatively, using the energy loss assumption from [Mayergoyz, 1991], the hysteretic loss is given by

$$\iint_\Omega \rho(\alpha,\beta)(\alpha-\beta) d\alpha d\beta, \tag{3.7}$$

where Ω is the region of points in the Preisach plane P for which the boundary of relays has changed during some input variation [Mayergoyz, 1991, p.46]; a typical shape of the region Ω is shown in Fig. 3.3. To formalize this notion let $\Omega := \Omega_\uparrow \cup \Omega_\downarrow$, where we the sub-regions $\Omega_\uparrow$ and $\Omega_\downarrow$ in the Preisach plane P whenever a switch in the relays occur from -1 to $+1$ for $\Omega_\uparrow$ and form $+1$ to -1 for $\Omega_\downarrow$ in the time interval $[t_i, t_{i+1}]$, i.e.,

$$\Omega_\uparrow := \Omega_{\uparrow[t_i,t_{i+1}]} = P_-(t_i) \cap P_+(t_{i+1}), \tag{3.8a}$$

$$\Omega_\downarrow := \Omega_{\downarrow[t_i,t_{i+1}]} = P_+(t_i) \cap P_-(t_{i+1}). \tag{3.8b}$$

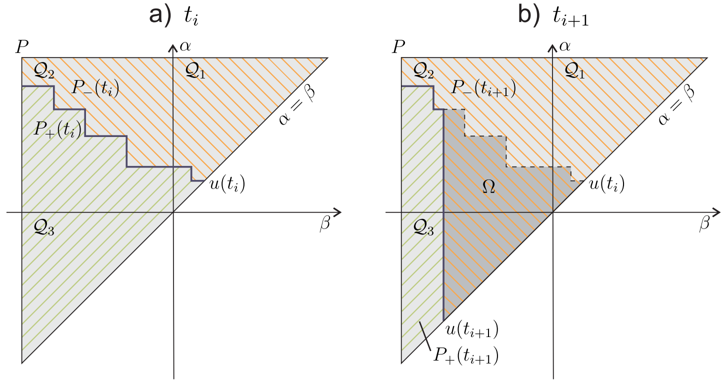

Figure 3.3: Preisach plane P, the Ω region, and the sub-regions P_+, P_-, $\mathcal{Q}_1$, $\mathcal{Q}_2$ and $\mathcal{Q}_3$ for a) t_i and b) t_{i+1}.

Following the evenly split energy loss assumption of [Mayergoyz, 1991], the dissipated energy between two consecutive time instances t_i and t_{i+1}, can be rewritten as

$$\begin{aligned}
\mathcal{D}_{[t_i,t_{i+1}]} := \mathcal{D}^u_{[t_i,t_{i+1}]} &= \iint\limits_{(\mathcal{Q}_1 \cup \mathcal{Q}_2 \cup \mathcal{Q}_3) \cap (\Omega_\uparrow \cup \Omega_\downarrow)} \frac{|q_\alpha + q_\beta|}{2} d\alpha d\beta, \\
&= \iint\limits_{P \cap (\Omega_\uparrow \cup \Omega_\downarrow)} \frac{2\rho(\alpha,\beta)(\alpha-\beta)}{2} d\alpha d\beta, \\
&= \iint\limits_{\Omega_{[t_i,t_{i+1}]}} \rho(\alpha,\beta)(\alpha-\beta) d\alpha d\beta, \qquad (3.9)
\end{aligned}$$

which corresponds to (3.7) for a time interval $[t_i, t_{i+1}]$. In the sequel the dissipated energy on an interval $[0,\eta]$ is considered to be given by $\mathcal{D}_{[0,\eta]} : u \mapsto \mathcal{D}^u_{[0,\eta]}$.

3.3 Dissipation and Damage

In natural sciences, hysteresis is often associated with irreversible thermodynamic changes. The second law of thermodynamics can be used to determine if a process is reversible or not; broadly speaking all real-life processes are non-reversible [Sears et al., 1982]. Accordingly, letting $\mathcal{D}$ be the dissipated energy, in the context of stress-strain relationships the second law of thermodynamics states that one can obtain the energy dissipation rate as

$$\dot{\mathcal{D}} = \dot{\epsilon}\sigma - \dot{V}, \quad \dot{\mathcal{D}} \geq 0, \qquad (3.10)$$

where ϵ is strain, σ is stress, and V corresponds to internal energy. Considering a Preisach hysteresis operator $\mathcal{W}$ one can write a stress-strain constitutive law as

$$\epsilon = \mathcal{W}[\sigma]. \qquad (3.11)$$

In general, even though dissipation is closely related to damage, whether they are proportional or positively correlated is not clear and has been much debated [Brokate et al., 1996]. In [Nagode & Zingsheim, 2004], a temperature modified strain-life approach using temperature is presented, based on a Prandtl operator; this strategy is also related to the rainflow counting procedure. In [Popov, 2010] the wear is proportional to dissipated energy in the context of contact mechanics.

Consider the damage in the rainflow counting sense in (2.11) but for functions instead of strings such that for a given signal u, the total damage D_{ac} on the time interval $[0, \eta]$ with $\eta \geq 0$ is given by

$$D_{ac}(u, \eta) := \sum_{\beta < \alpha} \frac{c(u, \alpha, \beta, \eta)}{\mathcal{N}(\alpha, \beta)}, \tag{3.12}$$

where $c(u, \alpha, \beta, \eta)$ is the rainflow count associated to u on $[0, \eta]$ and $\mathcal{N}(\alpha, \beta)$ denotes the number of cycles to failure. From Proposition 1 in the previous chapter, let $\Phi(u)$ be the Preisach operator in (2.9) with density function $\rho(\alpha, \beta) := -\frac{1}{2} \frac{\partial}{\partial\alpha\partial\beta} \left(\frac{1}{\mathcal{N}(\alpha,\beta)} \right)$. Then the following equivalency holds

$$D_{ac}(u, \eta) = \left| \Phi(u) \right|_{[0,\eta]}, \tag{3.13}$$

where $\left| \cdot \right|_{[0,\eta]}$ corresponds to the total variations in (3.2).

Proposition 2 (Variation and dissipated energy equivalence). [Barradas-Berglind et al., 2015a] *Let the input $u \in C_{pm}(\mathbb{R}_+)$. Consider the Preisach hysteresis operator Φ_1 defined as in* (2.9) *and the weighted Preisach hysteresis operator*

$$\Phi_2(u) = \int\limits_{\beta < \alpha} \hat{\rho}(\alpha, \beta) \mathcal{R}_{\beta,\alpha}(u) d\beta d\alpha, \tag{3.14}$$

with density function $\hat{\rho}(\alpha, \beta) = \frac{2\rho(\alpha,\beta)}{\alpha-\beta} = -\frac{\partial}{\partial\alpha} \frac{\partial}{\partial\beta} \left(\frac{1/\mathcal{N}(\alpha,\beta)}{\alpha-\beta} \right)$, where $\mathcal{N}(\alpha, \beta)$ is the number of cycles to failure. Then it follows that

$$D_{ac}(u, \eta) = \mathcal{D}_{[0,\eta]}\big(\Phi_2(u)\big) + c_1, \tag{3.15}$$

where c_1 is the initial condition of $\Phi_1(u)$.

3.4 Dissipation Theory Basics

Consider the non-linear system

$$\dot{x} = f(x, u), \tag{3.16a}$$
$$y = h(x, u), \tag{3.16b}$$

where $f \in \mathcal{C}^1(\mathbb{R}^n \times \mathbb{R}, \mathbb{R}^n)$ and $h \in \mathcal{C}^1(\mathbb{R}^m \times \mathbb{R}, \mathbb{R}^m)$ for bounded input u. Following [Willems, 1972], the notion of a dissipative system involves: a dynamical system such as (3.16), a supply rate $S : AC(\mathbb{R}) \times AC(\mathbb{R}) \to AC(\mathbb{R})$, and a storage function $H : \mathbb{R}^n \to \mathbb{R}$.

Definition 8 (Dissipation inequality). [Willems, 1972] *The system* (3.16) *is said to satisfy the dissipation inequality with respect to the supply rate S and the storage H if*

$$H\big(x(t_2)\big) - H\big(x(t_1)\big) \leq \int_{t_1}^{t_2} S\big(u(t), y(t)\big)\, dt \tag{3.17}$$

holds for all t_1, $t_2 \in \mathbb{R}$, with $t_2 \geq t_1$.

Definition 9 (Dissipative system). [Willems, 1972] *The system* (3.16) *is said to be dissipative with respect to the supply rate S if there exists a non-negative storage H such that the dissipation inequality* (3.17) *holds. If* (3.17) *holds with equality, then* (3.16) *is lossless with respect to S.*

In broad terms what Definition 9 entails is that when a system is dissipative, the stored energy is less that the energy supplied. Thus, some energy is lost or dissipated in the process.

3.5 Duhem Hysteresis and Dissipation

Based on the previous equivalences in Propositions 1 and 2 between damage and dissipation, one can see that the accumulated damage is has a connection to the amount of dissipated energy via the total variations. Accordingly, the dissipated energy of a different hysteresis operator can be studied in the sense of Definition 9, i.e., the Duhem hysteresis operator, which has the advantage of being represented by a differential equation instead of the Preisach hysteresis operator. The Duhem hysteresis model can be explicitly written as a differential equation, and focuses on the fact that the output can only change its character when the input changes direction [Macki et al., 1993]. Consequently, the Duhem model has scalar memory, i.e., it accesses information about past evolution through a single variable at each time, in contrast to the Preisach model that exhibits infinite dimensional memory [Brokate & Sprekels, 1996]. Using the same description as in [Macki et al., 1993, Visintin, 1994, Jayawardhana et al., 2012] the Duhem operator $\Phi : AC(\mathbb{R}_+) \times \mathbb{R}_+ \to AC(\mathbb{R}_+), (u, y_0) \mapsto \Phi(u, y_0) =: y$ is described by

$$\dot{y}(t) = f_1\big(y(t), u(t)\big)\dot{u}_+(t) + f_2\big(y(t), u(t)\big)\dot{u}_-(t), \tag{3.18a}$$

$$y(0) = y_0, \tag{3.18b}$$

where $\dot{u}_+(t) := \max\{0, \dot{u}(t)\}$, $\dot{u}_-(t) := \min\{0, \dot{u}(t)\}$ and $f_1, f_2 \in \mathcal{C}^1(\mathbb{R}^2)$. The existence of solutions to (3.18) has been addressed in [Macki et al., 1993].

As discussed in [Ouyang et al., 2013], the hysteretic phenomenon can be classified according to its input-output mapping into counter-clockwise (CCW), clockwise (CW) or more complex behavior. In Figure 3.4 the CW and CCW behavior of the Duhem semi-linear hysteresis model are shown. In the case of Preisach hysteresis in [Brokate & Sprekels, 1996, p.66] it is explained that whether this input-output behavior is CW or CCW, depends on the choice of the input variable. According to [Brokate & Sprekels, 1996], the constitutive law such as (3.11) with stress as input and strain as output gives rise to CCW loops. Hence, the CCW case is considered in the sequel.

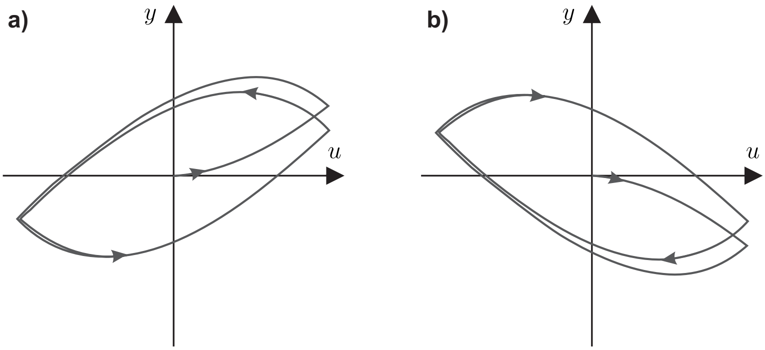

Figure 3.4: Duhem semi-linear hysteresis model input-output behavior from [Padthe et al., 2005] with sinusoidal input for a) counter clock-wise (CCW) and b) clock-wise (CW) orientation .

Definition 10 (Duhem model CCW dissipativity inequality). [Jayawardhana et al., 2012] *The Duhem operator as in* (3.18) *is said to be dissipative with respect to the supply rate $S(u, y) = \dot{y}u$ if there exists a non-negative function $H : \mathbb{R}^2 \to \mathbb{R}_+$ such that for every $u \in AC(\mathbb{R}_+)$ and $y_0 \in \mathbb{R}$*

$$\frac{dH(y(t), u(t))}{dt} \leq \dot{y}(t)u(t) \tag{3.19}$$

holds for almost all $t \in \mathbb{R}_+$ with $y := \Phi(u, y_0)$.

If one considers H as defined in Definition 10 as being the stored energy in the system, the inequality (3.19) can be interpreted as the exchange of energy with the environment where the supplied energy given by $\int_0^T \dot{y}(\tau)u(\tau)d\tau$ is subtracted by a non-negative quantity, namely the *dissipated energy*.

Definition 11 (Duhem CCW Dissipated energy). *For the Duhem hysteresis model Φ with $y = \Phi(u)$, the dissipated energy $\mathcal{D} : AC(\mathbb{R}_+) \times AC(\mathbb{R}_+) \to AC(\mathbb{R}_+)$ for the CCW case is defined by*

$$\mathcal{D}_{[0,t]}(y, u) = \int_0^t \dot{y}(\tau)u(\tau)d\tau - H\big(y(t), u(t)\big) + H\big(y(0), u(0)\big). \tag{3.20}$$

It is immediate to check that $\dot{\mathcal{D}}_{[0,t]}(y, u) \geq 0$ for all t, or in other words the dissipated energy is a non-decreasing function along the trajectory of y and u. Notice the relationship of this property to the dissipated energy of the Preisach model, and consequently to damage in the rainflow counting sense as exploited in [Paper E–F].

4 Damage Reduction Wind Turbine Control Strategies

"He who would learn to fly one day must first learn to stand and walk and run and climb and dance; one cannot fly into flying."

~Friedrich Nietzsche

This chapter presents a summary of the fatigue-damage reduction control strategies proposed in this thesis. These contributions correspond to [Paper B–G]. The strategies in [Paper B–F] correspond to the wind turbine level, whereas the strategy proposed in [Paper G] is on the wind farm level.

In this chapter a total of four fatigue-damage reduction control strategies are summarized. The first three strategies are focused in the turbine level and strive to reduce the damage in the drive-train. Additionally, a fourth strategy dedicated to wind farm mixed-objective operation optimization is presented.

4.1 Wind Turbine Level Control Strategies

Consider a wind turbine plant model $\mathcal{P}$ as described in Section 1.3 and an exogenous wind input v_r seen as a disturbance and operating in full-load or Region 3, according to Figure 1.4. Consequently, the goal is to design a control strategy $\mathcal{C}$ that reduces the damage in certain component of the wind turbine, while it maintains the power output and reduces its deviations. For controller design purposes in the wind turbine level —the plant dynamics to be used for controller synthesis— only the rotational mode of the shaft is considered, namely the drive-train system described by the following set of differential equations

$$J_r\dot{\omega}_r = T_r(\lambda, \beta_p) - K_\theta\theta - B_\theta\dot{\theta}, \tag{4.1a}$$

$$J_g\dot{\omega}_g = -T_g + \frac{K_\theta}{N_g}\theta + \frac{B_\theta}{N_g}\dot{\theta}, \tag{4.1b}$$

$$\dot{\theta} = \omega_r - \frac{\omega_g}{N_g}, \tag{4.1c}$$

where ω_r corresponds to the rotor angular velocity, ω_g to the generator angular velocity, and θ to the shaft torsion. In addition, T_g is the generator torque and $T_r(\lambda, \beta_p)$ is the aerodynamic rotor torque, which is a function of the collective pitch angle β_p and the tip speed ratio $\lambda(\omega_r, v_r) := R_r\omega_r/v_r$. Moreover, R_r, N_g, K_θ, B_θ, J_r, and J_g are constants. Further details about the model can be found in [Paper B–C, E–F].

Remark 3*: Here it is assumed that the controller has full access to all states, i.e., generator speed ω_g, rotor speed ω_r and shaft torsion θ. Additionally, the dynamics in* (4.1) *are linearized at a chosen operating point according to the main wind speed, and the wind residual (after subtracting the mean) is seen as a disturbance.*

Consequently, the intention is to characterize the fatigue-damage in the drive-train and the focus of this thesis is on the damage reduction in this particular component, which is realized by inspecting the shaft torsion θ. This is relevant since the maintenance costs for the drive-train —gearbox, main shaft, and bearings— are quite significant, as shown in Figure 1.3, amounting to around half the maintenance costs for that example.

In the sequel three different drive-train fatigue-damage reduction strategies are presented:

- $\mathcal{C}_1$: via recursive least-squares estimation
- $\mathcal{C}_2$: for DLTI systems with Preisach hysteresis output
- $\mathcal{C}_3$: through hysteresis dissipated energy

These control strategies are all optimization based and are implemented in receding horizon fashion, being formulated as modified or augmented model predictive (MPC) strategies. These algorithms rely on MPC since it is a well-known and developed control strategy which can accommodate in different ways (although not directly) the damage estimation provided by the hysteresis operators [Maciejowski, 2002, Camacho & Bordons, 2004]. Moreover, constraints can be handled directly which is relevant for pitch angle and generator torque, and it has been successfully used for wind turbine control. MPC is an optimization based control technique widely used for controller design of complex systems. The main idea behind MPC is to use the plant dynamics to predict the state evolution, and together with a cost functional obtain a constrained optimal control problem. At a given time step, solving this control problem provides an optimal control sequence from which only the first is implemented in receding horizon fashion. Subsequently, the same process is repeated for the next time steps [Maciejowski, 2002, Camacho & Bordons, 2004].

In general terms, problems involving hysteresis are hard, since hysteresis operators involve discontinuities and non-smooth non-linearities, and in the case of the Preisach hysteresis model, infinite dimensional memory [Brokate & Sprekels, 1996]. Therefore, the proposed strategies in $\mathcal{C}_1$ and $\mathcal{C}_2$ used the discretized version of the Preisach hysteresis instead of the infinite-dimensional one. Moreover, $\mathcal{C}_1$ relies in a further approximation via least-squares. Lastly, in the case of $\mathcal{C}_3$ a choice in the stress-strain relationship was made to characterize the input-output direction and a semi-linear model was used. These strategies are summarized in the following subsections.

4.1.1 Damage Reduction via Recursive Least-Squares

Firstly, consider that the damage is provided by the variations of a Preisach operator acting on the shaft torsion, i.e., $\text{Var}\big(\mathcal{H}(\theta)\big)$ where $\text{Var}(\cdot)$ corresponds to the variation operator in (2.12) and $\mathcal{H}$ is the discretized Preisach hysteresis operator from (2.9).

Subsequently, there is a damage estimator $\mathcal{LS}$ whose aim is to approximate the damage in the shaft as best as possible in the least-squares sense. Thus, the least-squares based estimator $\mathcal{LS}$ provides the adaptive coefficients $(\hat{a}, \hat{g})$ to the controller $\mathcal{C}_1$ (described in detail in [Paper B–C]). The controller or damage reduction control strategy $\mathcal{C}_1$ is a convex optimization based algorithm that incorporates $(\hat{a}, \hat{g})$ through its cost functional, and is synthesized using CVX [Grant & Boyd, 2014]. As sketch diagram of this strategy is depicted in Figure 4.1.

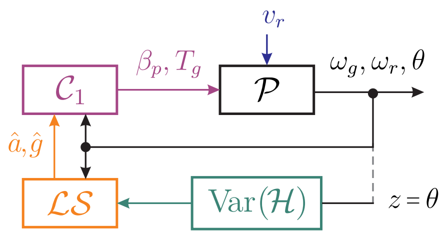

Figure 4.1: Damage reduction control strategy via least-squares based on a Preisach hysteresis operator.

The fact that the variation operator is present is key in the design of the estimator $\mathcal{LS}$, since it introduces a type of integral action, which makes the approximation possible. The control strategy is guaranteed to remain convex for $\hat{a}, \hat{g} > 0$, as shown in [Paper B–C]. Stability then follows for model predictive controllers with quadratic costs and linear constraints [Mayne et al., 2000, Maciejowski, 2002].

4.1.2 Damage Reduction for DLTI systems with Preisach hysteresis output

In order to avoid the least-squares approximation used to synthesize $\mathcal{C}_1$, the discretized Preisach operator can be cast in the mixed logical dynamical (MLD) systems framework introduced in [Bemporad & Morari, 1999], which can be used to describe a gamut of systems with dynamic equations subject to linear inequalities involving real and integer variables. Accordingly, the augmented plant $\mathcal{P}_{aug}$ is a MLD system that includes the discretized and linearized plant $\mathcal{P}$ with discretized Preisach hysteresis output, i.e., with $\mathcal{H}$ being the discretized Preisach hysteresis operator from (2.9). Hence, the augmented MLD plant $\mathcal{P}_{aug}$ provides the controller $\mathcal{C}_2$ with the damage output on the shaft $\mathcal{H}(\theta)$; the HYSDEL compiler [Torrisi & Bemporad, 2004] was used to translate the plant dynamics and constraints into the MLD formalism.

In this case the controller or damage reduction control strategy $\mathcal{C}_2$ is a mixed-integer optimization algorithm that incorporates the shaft torsion damage in the cost functional. This optimization problem is solved using the Hybrid Toolbox [Bemporad,

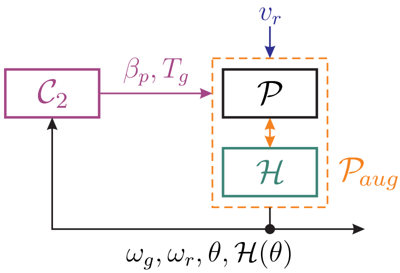

Figure 4.2: Damage reduction control strategy for systems with Preisach hysteresis output.

2003] which translates the problem into a mixed integer program (MIP). As sketch diagram of this strategy is depicted in Figure 4.2; this strategy is discussed in greater detail in [Paper D]. Note that complexity quickly escalates when the number of relays in the discretized Preisach hysteresis increases.

Remark 4*: The MLD formalism does not handle disturbances directly, so in order to include the wind disturbance v_r two models were used, i.e., one for controller synthesis with two inputs, and a second one for simulation with three inputs where v_r is injected as an exogenous input. Alternatively, one could include a wind estimator or a disturbance model, which would result in an increased number of states.*

4.1.3 Damage Reduction through Dissipated Energy

For this damage reduction strategy the notion of damage in the rainflow counting sense is transported to dissipated energy, as discussed in Section 3.3. Let Φ be a Duhem hysteresis operator with input $z = \theta$ and output $y = \Phi(z)$; in addition, let its dissipated energy be characterized by $\mathcal{D}(z, y)$ as in (3.20). The Duhem hysteresis model (3.18) has the advantage that it can be explicitly written as a differential equation. This is due to the fact that the Duhem hysteresis model has scalar memory, contrary to the Preisach hysteresis infinite dimensional memory, which facilitates its inclusion in the optimization problem.

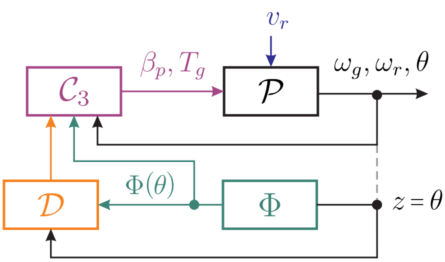

Figure 4.3: Damage reduction control strategy through dissipated energy.

The control scheme is sketched in Figure 4.3, where it can be appreciated that the control strategy receives the states, the Duhem hysteresis output and the dissipated energy. Consequently, $\mathcal{C}_3$ is a non-linear MPC strategy where Φ is chosen as a semi-linear Duhem model that can be described as a switched system; [Paper E–F] present this strategy is more detail. The controller was synthesized using `Yalmip` [Löfberg, 2004] with the `BNB` solver. The optimization problem has a quadratic cost functional that is guaranteed to be positive, but the problem is non-convex due to the Duhem hysteresis dynamics.

4.1.4 Strategies Comparison

Three different drive-train fatigue-damage reduction wind turbine control strategies are proposed in this thesis. The control strategies $\mathcal{C}_2$ and $\mathcal{C}_3$ are of a non-convex nature (note that convexification methods [Tawarmalani & Sahinidis, 2002] could be used to relax the mixed integer problem), whereas $\mathcal{C}_1$ is convex. As it is well-known, convexity is a desired property for which tools are available that guarantee good computational time; contrastingly, non-convex (mixed integer) problems are harder to solve for which computational time rapidly escalates. This is also reflected in the horizon that can be used in the optimization problem. In terms of complexity, $\mathcal{C}_1$ is the leanest, followed by $\mathcal{C}_3$, and lastly $\mathcal{C}_2$ where constraints pertaining to auxiliary variables build up rapidly.

The main advantage of $\mathcal{C}_1$ is that it is a convex solution with recursive adaption, with the downside that the structure of the damage was assumed to be proportional to the shaft torsion squared and its derivative squared. Subsequently, the main advantage of $\mathcal{C}_2$ is that the Preisach output can be directly used in the cost functional, but the non-convexity of the problem and the dimensionality of the MLD structure limit the number of relays that can be included; furthermore, a wind estimator may be needed, which will also add to the number of states. One of the main advantages of $\mathcal{C}_3$ is that dissipation theory is very well developed for control purposes; in addition, the Duhem hysteresis can be written down as a differential equation and it can be used in several application domains. However, some disadvantages of $\mathcal{C}_3$ are that the relationship between the Preisach and Duhem operators dissipation needs to be further studied — perhaps considering other Duhem models and not only the semi-linear one— and that the optimization problem remains non-convex.

4.2 Wind Farm Mixed-Objective Operation Optimization

The previous section focused on the proposed control strategies for the wind turbine level. This section focuses on the contribution of this thesis corresponding to the wind farm level. In this case an array of $1 \leq i \leq N$ wind turbines is considered as depicted in Figure 4.4, described by the actuator disc model [Bianchi et al., 2006].

Consider that each wind turbine receives an input wind flow v_i and performs a control action a_i — known as the axial-induction factor, which can be controlled by either the generator torque T_g or the pitch angle β_p [Johnson & Thomas, 2009]. Accordingly, each wind turbine generates certain amount of power P_i; furthermore, each turbine experiences certain thrust force F_i with force deviations Υ_i characterizing the

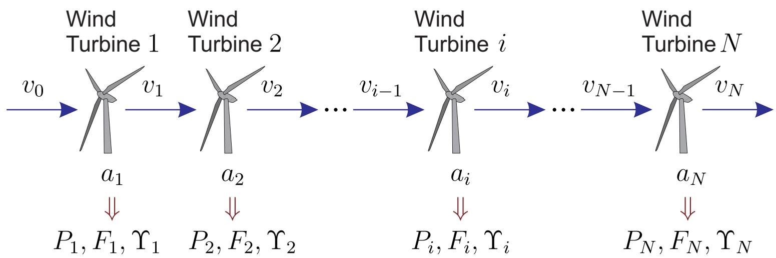

Figure 4.4: Damage reduction control strategy through dissipated energy.

mechanical loads. The proposed mixed-objective wind farm optimization strategy in [Paper G] is given by the solution of the following maximization problem

$$\max_a \sum_{i=1}^{N} P_i - \xi \sum_{i=1}^{N} F_i - \lambda \sum_{i=1}^{N} \Upsilon_i, \tag{4.2}$$

where $a = \{a_1, a_2, \cdots, a_N\}$ corresponds to the control action of each turbine, and ξ, λ are positive scalars describing the balance between power and load reduction that can be thought of as risk aversion weightings. It would make good sense to choose ξ and λ according to the electricity market conditions, effectively allowing the wind farm operator to boost power production when necessary and to save in mechanical loads otherwise. Further details and numerical examples are given in [Paper G].

Compared to regular power maximization wind farm strategies, the strategy in (4.2) allows for different ways of operating the wind turbine depending on whether power output or infrastructure wear is more important. In the special case when $\xi, \lambda = 0$, the proposed strategy in (4.2) becomes a purely power maximization strategy as the ones described in [Bitar & Seiler, 2013, Rotea, 2014].

4.3 Discussion

Three different damage reduction control strategies in the wind turbine level were sketched and their advantages, disadvantages and respective complexity were discussed. Additionally, a mixed-objective optimization operation strategy in the wind farm level was presented. All four strategies are aligned with the wind energy conversion systems control objectives described in Section 1.2. Specifically, the main focus was on integrating the mechanical load minimization into the optimization problems.

These strategies add findings to the current insight of fatigue-damage estimation in wind energy conversion systems by addressing the aforementioned trade-off between power maximization and mechanical loads minimization.

5 | Closing Remarks

> *"Temet nosce (Know thyself)"*
>
> *~Delphic maxim inscribed in the Temple of Apollo*
>
> *This final chapter of the first part of this thesis presents the conclusions of the work. In addition, perspectives and recommendations are given based on the investigation conducted.*

5.1 Conclusions

The recent developments in the smart grid and in the wind energy industry in general motivate the consideration of control strategies involving the wind energy conversion mixed control objective, i.e., power maximization and mechanical load alleviation, instead of solely concentrating in maximum generation. This is especially relevant in the presence of electricity markets, where price exhibits fluctuations and dips. Fatigue-damage is a critical factor in wind turbines since it is necessary to ensure a fixed minimal life span under both normal and transient operating conditions in a turbulent environment. Damage is caused by loading on a material structure resulting in deformations or cracks, compromising its integrity as a result. Accordingly, fatigue-damage estimation plays a central role in this thesis with special focus on its inclusion in wind turbine control strategies.

Firstly, in this thesis a comprehensive exposition of fatigue-damage estimation methods in the component level was given, including a comparison amongst them together with discussion about their underlying relationships and their applicability to control of wind turbines, in an effort to elucidate the role of fatigue-damage estimation in control loops.

Subsequently, three different drive-train fatigue-damage reduction predictive control strategies for wind turbines were proposed, based on hysteresis operators and focused on online fatigue-damage estimation. The first one is a convex adaptive strategy based on parameter identification of previous measurement data via least-squares estimation. The second strategy leans on the mixed logical dynamical (MLD) systems formalism to include the fatigue-damage estimation as an augmented plant model, and consequently an integer optimization problem can be formulated. Lastly, the third control strategy incorporates the dissipated energy of a scalar hysteresis operator that models the stress-strain behavior.

Additionally, a mixed-objective wind farm operation optimization strategy was proposed, which effectively allows the wind farm operator to boost power production when necessary and to take care of infrastructure wear otherwise. This is of particular interest when considering integration with the electricity market.

In summary, and in line with the hypotheses introduced at the beginning of this thesis, the most relevant methods for fatigue-damage estimation were explored, and accordingly damage proxies of the drive-train were included in the wind turbine control problem. Finally, the mixed-objective optimization problem for the wind farm level operation was addressed.

5.2 Perspectives and Recommendations

After this investigation the following recommendations for control of wind energy conversion systems can be provided:

- The proposed least-squares recursive estimation based on the variations of a Preisach hysteresis operator in [Paper B–C], depends on the squared shaft torsion and the squared derivative of the shaft torsion. Practically, this is similar to include certain number of moments that characterize the loading. Accordingly, this could be extended by considering higher order moments.

- Regarding the control strategy proposed in [Paper D], as pointed out in Remark 4, the MLD formalism does not handle disturbances directly. This leads to two perspectives: the first one is the inclusion of wind estimation as part of the augmented plant; the second one is the analysis of the parametrization of MLD systems as a function of some exogenous variable (such as the wind) in order to accommodate different operating points (according to wind speeds) similar to what is done when considering a linear parameter varying (LPV) system.

- The primary focus of this thesis is on the drive-train damage, and thus only the rotational mode of the shaft was considered for controller design. Extension of the number of states, such as tower dynamics and pitch actuator may improve the results.

- The wind farm operation optimization strategy in [Paper G] relies on the assumption that extreme loads are captured by the mean and fatigue damage by the variance. This may not always be the case; however, additional moments could be integrated in the optimization problem. Alternatively, the problem could be addressed from a stochastic perspective considering a wind distribution.

Finally, on a more general tone the following perspectives and recommendations are given:

- In [Paper E–F] the relationships between variations, damage and dissipation for the Preisach hysteresis were explored. Additionally, this notion was transported to the Duhem hysteresis model. The results in [Paper E–F] suggest that further analysis is needed to determine the exact relationship between dissipation in the

Preisach and the Duhem models, and perhaps consider different Duhem models other than the semi-linear one.

- Fatigue-damage is a very relevant factor for market integration of wind energy generating systems. Currently, as such, fatigue-damage is an a-priori stipulation. A holistic approach may be needed to consider not only power maximization and fatigue-damage reduction, but also extreme loads, transient phenomena and economical and operational issues as a whole.

- The inclusion of the grid operator requests or demands in the wind farm optimization was not considered in this thesis. This could be achieved for instance by adapting the weightings in the control strategy optimization problem. However, this poses another trade-off between fulfilling the grid requirements and the wind farm business case.

- A formal way of adjusting the trade-off weightings in [Paper G] could be investigated. One possibility is to set those weightings according to financial considerations, e.g., in terms of the price of electricity, the expected return, and the tolerable risk —comparable to Markowitz portfolio analysis [Markowitz, 1952].

References

[Adegas et al., 2012] Adegas, F. D., Sloth, C., & Stoustrup, J. (2012). Structured linear parameter varying control of wind turbines. In *Control of Linear Parameter Varying Systems with Applications* (pp. 303–337). Springer.

[Adegas et al., 2013] Adegas, F. D., Wisniewski, R., & Sloth Larsen, L. F. (2013). Gain-scheduled model predictive control of wind turbines using laguerre functions. In *American Control Conference (ACC), 2013* (pp. 653–658).: IEEE.

[Albadi & El-Saadany, 2008] Albadi, M. H. & El-Saadany, E. (2008). A summary of demand response in electricity markets. *Electric power systems research*, 78(11), 1989–1996.

[Annoni et al., 2015] Annoni, J., Gebraad, P. M., Scholbrock, A. K., Fleming, P. A., & van Wingerden, J.-W. (2015). Analysis of axial-induction-based wind plant control using an engineering and a high-order wind plant model. *Wind Energy*.

[Barradas-Berglind et al., 2015a] Barradas-Berglind, J., Jayawardhana, B., & Wisniewski, R. (2015a). Energy dissipation in hysteresis models for wind turbine control damage reduction. *Submitted to IEEE Transactions on Control Systems Technology*.

[Barradas-Berglind et al., 2015b] Barradas-Berglind, J., Jayawardhana, B., & Wisniewski, R. (2015b). Wind turbine control with active damage reduction through energy dissipation. In *Submitted to the 2016 American Control Conference (ACC)*.

[Barradas-Berglind & Wisniewski, 2015a] Barradas-Berglind, J. & Wisniewski, R. (2015a). Control of linear systems with preisach hysteresis output with application to damage reduction. In *14th European Control Conference (ECC)* (pp. 3577–3583).

[Barradas-Berglind & Wisniewski, 2015b] Barradas-Berglind, J. & Wisniewski, R. (2015b). Representation of fatigue for wind turbine control. *Submitted to Wind Energy*.

[Barradas-Berglind & Wisniewski, 2015c] Barradas-Berglind, J. & Wisniewski, R. (2015c). Wind farm axial-induction factor optimization for power maximization and load alleviation. In *Submitted to the 15th European Control Conference (ECC)*.

[Barradas-Berglind et al., 2015c] Barradas-Berglind, J., Wisniewski, R., & Soltani, M. (2015c). Fatigue damage estimation and data-based control for wind turbines. *IET Control Theory & Applications*, 9(7), 1042–1050.

[Barradas-Berglind et al., 2015d] Barradas-Berglind, J., Wisniewski, R., & Soltani, M. (2015d). Fatigue load modeling and control for wind turbines based on hysteresis operators. In *2015 American Control Conference (ACC)* (pp. 3721–3727).

[Bemporad, 2003] Bemporad, A. (2003). Hybrid Toolbox-user\'s guide.

[Bemporad & Morari, 1999] Bemporad, A. & Morari, M. (1999). Control of systems integrating logic, dynamics, and constraints. *Automatica*, 35(3), 407–427.

[Bianchi et al., 2006] Bianchi, F. D., De Battista, H., & Mantz, R. J. (2006). *Wind turbine control systems: principles, modelling and gain scheduling design*. Springer Science & Business Media.

[Bitar & Seiler, 2013] Bitar, E. & Seiler, P. (2013). Coordinated control of a wind turbine array for power maximization. In *American Control Conference (ACC), 2013* (pp. 2898–2904).: IEEE.

[Blaabjerg et al., 2012] Blaabjerg, F., Liserre, M., & Ma, K. (2012). Power electronics converters for wind turbine systems. *IEEE Transactions on Industry Applications*, 48(2), 708–719.

[Bogsjö & Rychlik, 2009] Bogsjö, K. & Rychlik, I. (2009). Vehicle fatigue damage caused by road irregularities. *Fatigue & Fracture of Engineering Materials & Structures*, 32(5), 391–402.

[Bossanyi, 2000] Bossanyi, E. (2000). The design of closed loop controllers for wind turbines. *Wind Energy*, 3(3), 149–163.

[Bossanyi, 2003] Bossanyi, E. (2003). Wind turbine control for load reduction. *Wind Energy*, 6(3), 229–244.

[Bossanyi, 2005] Bossanyi, E. (2005). Further load reductions with individual pitch control. *Wind Energy*, 8(4), 481–485.

[Brodtkorb et al., 2000] Brodtkorb, P., Johannesson, P., Lindgren, G., Rychlik, I., Rydén, J., & Sjö, E. (2000). WAFO - a Matlab toolbox for the analysis of random waves and loads. In *Proc. 10'th Int. Offshore and Polar Eng. Conf., ISOPE, Seattle, USA*, volume 3 (pp. 343–350).

[Brokate et al., 1996] Brokate, M., Dreßler, K., & Krejčí, P. (1996). Rainflow counting and energy dissipation for hysteresis models in elastoplasticity. *European Journal of Mechanics A/Solids*, 15(4), 705–737.

[Brokate & Sprekels, 1996] Brokate, M. & Sprekels, J. (1996). *Hysteresis and phase transitions, volume 121 of Applied Mathematical Sciences*. Springer-Verlag, New York.

[Callaway & Hiskens, 2011] Callaway, D. S. & Hiskens, I. (2011). Achieving controllability of electric loads. *Proceedings of the IEEE*, 99(1), 184–199.

[Camacho & Bordons, 2004] Camacho, E. F. & Bordons, C. (2004). *Model Predictive Control*, volume 2. Springer.

[Chen et al., 2009] Chen, Z., Guerrero, J. M., & Blaabjerg, F. (2009). A review of the state of the art of power electronics for wind turbines. *IEEE Transactions on Power Electronics*, 24(8), 1859–1875.

[Coleman & Hodgdon, 1987] Coleman, B. D. & Hodgdon, M. L. (1987). On a class of constitutive relations for ferromagnetic hysteresis. *Archive for Rational Mech. and analysis*, 99(4), 375–396.

[Dahl, 1976] Dahl, P. R. (1976). Solid friction damping of mechanical vibrations. *AIAA Journal*, 14(12), 1675–1682.

[De Wit et al., 1995] De Wit, C. C., Olsson, H., Astrom, K. J., & Lischinsky, P. (1995). A new model for control of systems with friction. *IEEE Trans. Aut. Control*, 40(3), 419–425.

[Downing & Socie, 1982] Downing, S. & Socie, D. (1982). Simple rainflow counting algorithms. *International Journal of Fatigue*, 4(1), 31–40.

[Doyle et al., 2013] Doyle, J. C., Francis, B. A., & Tannenbaum, A. R. (2013). *Feedback control theory*. Courier Corporation.

[Edlund et al., 2011] Edlund, K., Bendtsen, J. D., & Jørgensen, J. B. (2011). Hierarchical model-based predictive control of a power plant portfolio. *Control Engineering Practice*, 19(10), 1126–1136.

[Endo et al., 1967] Endo, T., Mitsunaga, K., & Nakagawa, H. (1967). Fatigue of metals subjected to varying stress-prediction of fatigue lives. In *Preliminary Proc. of the Chugoku-Shikoku District Meeting* (pp. 41–44).

[Energinet.dk, 2014] Energinet.dk (2014). Technical regulations. `http://www.energinet.dk/EN/El/Forskrifter/Technical-regulations/Sider/default.aspx`.

[ENTSO-E, 2015] ENTSO-E (2015). Continental Europe Operation Handbook. `http://www.entsoe.eu/publications/system-operations-reports/operation-handbook/Pages/default.aspx`.

[ESGTP, 2006] ESGTP (2006). Vision and strategy for European electricity networks of the future. European SmartGrids Technology Platform.

[EWEA, 2007] EWEA (2007). Wind directions, Jan-Feb 2007. European Wind Energy Association.

[Farhangi, 2010] Farhangi, H. (2010). The path of the smart grid. *Power and Energy Magazine, IEEE*, 8(1), 18–28.

[Fleming et al., 2014] Fleming, P. A., Gebraad, P. M., Lee, S., van Wingerden, J.-W., Johnson, K., Churchfield, M., Michalakes, J., Spalart, P., & Moriarty, P. (2014). Evaluating techniques for redirecting turbine wakes using SOWFA. *Renewable Energy*, 70, 211–218.

[Franz, 1990] Franz, W. (1990). *Hysteresis in economic relationships: An overview*. Springer.

[Friis et al., 2011] Friis, J., Nielsen, E., Bonding, J., Adegas, F. D., Stoustrup, J., & Odgaard, P. F. (2011). Repetitive model predictive approach to individual pitch control of wind turbines. In *50th CDC-ECC* (pp. 3664–3670).: IEEE.

[Gebraad et al., 2014] Gebraad, P., Teeuwisse, F., van Wingerden, J., Fleming, P., Ruben, S., Marden, J., & Pao, L. (2014). Wind plant power optimization through yaw control using a parametric model for wake effects-a CFD simulation study. *Wind Energy*.

[Gorbet, 1998] Gorbet, R. B. (1998). *Control of hysteretic systems with Preisach representations.* PhD thesis, University of Waterloo.

[Gorbet et al., 2001] Gorbet, R. B., Morris, K. A., & Wang, D. W. (2001). Passivity-based stability and control of hysteresis in smart actuators. *IEEE Transactions on Control Systems Technology*, 9(1), 5–16.

[Grant & Boyd, 2014] Grant, M. & Boyd, S. (2014). CVX: Matlab software for disciplined convex programming, version 2.1. http://cvxr.com/cvx.

[GWEC, 2014] GWEC (2014). Global statistics. global wind energy council. `http://www.gwec.net/global-figures/graphs/`.

[Hammerum et al., 2007] Hammerum, K., Brath, P., & Poulsen, N. K. (2007). A fatigue approach to wind turbine control. In *J. of Physics: Conf. Series*, volume 75 (pp. 012–081).

[Hansen et al., 2006] Hansen, M. O. L., Sørensen, J. N., Voutsinas, S., Sørensen, N., & Madsen, H. A. (2006). State of the art in wind turbine aerodynamics and aeroelasticity. *Progress in aerospace sciences*, 42(4), 285–330.

[Herzog et al., 2007] Herzog, F., Dondi, G., & Geering, H. P. (2007). Stochastic model predictive control and portfolio optimization. *International Journal of Theoretical and Applied Finance*, 10(02), 203–233.

[Jayawardhana et al., 2008] Jayawardhana, B., Logemann, H., & Ryan, E. P. (2008). PID control of second-order systems with hysteresis. *International Journal of Control*, 81(8), 1331–1342.

[Jayawardhana et al., 2012] Jayawardhana, B., Ouyang, R., & Andrieu, V. (2012). Stability of systems with the Duhem hysteresis operator: The dissipativity approach. *Automatica*, 48(10), 2657–2662.

[Jiles & Atherton, 1986] Jiles, D. & Atherton, D. (1986). Theory of ferromagnetic hysteresis. *J. of Magnetism and Magnetic Materials*, 61(1), 48–60.

[Johnson & Fritsch, 2012] Johnson, K. & Fritsch, G. (2012). Assessment of extremum seeking control for wind farm energy production. *Wind Engineering*, 36(6), 701–716.

[Johnson et al., 2006] Johnson, K. E., Pao, L. Y., Balas, M. J., & Fingersh, L. J. (2006). Control of variable-speed wind turbines: standard and adaptive techniques for maximizing energy capture. *Control Systems, IEEE*, 26(3), 70–81.

[Johnson & Thomas, 2009] Johnson, K. E. & Thomas, N. (2009). Wind farm control: addressing the aerodynamic interaction among wind turbines. In *2009 American Control Conference (ACC)* (pp. 2104–2109).: IEEE.

[Jonkman & Buhl Jr, 2005] Jonkman, J. M. & Buhl Jr, M. L. (2005). Fast user's guide. *National Renewable Energy Laboratory, Technical Report No. NREL/EL-500-38230*.

[Jonkman et al., 2009] Jonkman, J. M., Butterfield, S., Musial, W., & Scott, G. (2009). *Definition of a 5-MW reference wind turbine for offshore system development*. National Renewable Energy Laboratory.

[Knudsen et al., 2014] Knudsen, T., Bak, T., & Svenstrup, M. (2014). Survey of wind farm control-power and fatigue optimization. *Wind Energy*.

[Krasnosel'skiĭ & Pokrovskiĭ, 1989] Krasnosel'skiĭ, M. A. & Pokrovskiĭ, A. V. (1989). *Systems with hysteresis*. Springer Verlag.

[Krupp, 2007] Krupp, U. (2007). *Fatigue crack propagation in metals and alloys: microstructural aspects and modelling concepts*. John Wiley & Sons.

[Kundur et al., 1994] Kundur, P., Balu, N. J., & Lauby, M. G. (1994). *Power system stability and control*, volume 7. McGraw-hill New York.

[Larsen et al., 2005] Larsen, T. J., Madsen, H. A., & Thomsen, K. (2005). Active load reduction using individual pitch, based on local blade flow measurements. *Wind Energy*, 8(1), 67–80.

[Litos, 2008] Litos, S. (2008). The smart grid: An introduction. Litos Strategic Communication for the U.S. Department of Energy.

[Löfberg, 2004] Löfberg, J. (2004). YALMIP: A toolbox for modeling and optimization in MATLAB. In *Proc. of the CACSD Conference* Taipei, Taiwan.

[Logemann & Ryan, 2003] Logemann, H. & Ryan, E. P. (2003). Systems with hysteresis in the feedback loop: existence, regularity and asymptotic behaviour of solutions. *ESAIM: Control, Opt. and Calc. of Var.*, 9, 169–196.

[Maciejowski, 2002] Maciejowski, J. M. (2002). *Predictive control: with constraints*. Pearson Education.

[Macki et al., 1993] Macki, J. W., Nistri, P., & Zecca, P. (1993). Mathematical models for hysteresis. *SIAM review*, 35(1), 94–123.

[Malhame & Chong, 1985] Malhame, R. & Chong, C.-Y. (1985). Electric load model synthesis by diffusion approximation of a high-order hybrid-state stochastic system. *IEEE Transactions on Automatic Control*, 30(9), 854–860.

[Markowitz, 1952] Markowitz, H. (1952). Portfolio selection. *The Journal of Finance*, 7(1), 77–91.

[Martin-Tretton et al., 2012] Martin-Tretton, M., Reha, M., Drunsic, M., & Keim, M. (2012). Data collection for current US wind energy projects: Component costs, financing, operations, and maintenance. NREL.

[Mayergoyz, 1991] Mayergoyz, I. D. (1991). *Mathematical Models of Hysteresis*. Springer-Verlag.

[Mayne et al., 2000] Mayne, D. Q., Rawlings, J. B., Rao, C. V., & Scokaert, P. O. (2000). Constrained model predictive control: Stability and optimality. *Automatica*, 36(6), 789–814.

[Miner, 1945] Miner, M. (1945). Cumulative damage in fatigue. *Journal of Applied Mechanics*, 12(3), 159–164.

[Mirzaei et al., 2013] Mirzaei, M., Soltani, M., Poulsen, N. K., & Niemann, H. H. (2013). Model predictive control of wind turbines using uncertain LIDAR measurements. In *2013 American Control Conference (ACC)* (pp. 2235–2240).

[Molderink et al., 2010] Molderink, A., Bakker, V., Bosman, M. G., Hurink, J. L., & Smit, G. J. (2010). Management and control of domestic smart grid technology. *IEEE Transactions on Smart grid*, 1(2), 109–119.

[Munteanu et al., 2008] Munteanu, I., Bratcu, A. I., Cutululis, N.-A., & Ceanga, E. (2008). *Optimal control of wind energy systems: towards a global approach*. Springer Science & Business Media.

[Nagode & Zingsheim, 2004] Nagode, M. & Zingsheim, F. (2004). An online algorithm for temperature influenced fatigue–life estimation: strain–life approach. *International Journal of Fatigue*, 26(2), 155–161.

[Odgaard et al., 2013] Odgaard, P. F., Stoustrup, J., & Kinnaert, M. (2013). Fault-tolerant control of wind turbines: A benchmark model. *IEEE Transactions on Control Systems Technology*, 21(4), 1168–1182.

[Ouyang et al., 2013] Ouyang, R., Andrieu, V., & Jayawardhana, B. (2013). On the characterization of the Duhem hysteresis operator with clockwise input–output dynamics. *Sys. & Control Lett.*, 62(3), 286–293.

[Padthe et al., 2005] Padthe, A., Oh, J., & Bernstein, D. S. (2005). Counterclockwise dynamics of a rate-independent semilinear Duhem model. In *44th IEEE Decision and Control and European Control Conf. (CDC-ECC)* (pp. 8000–8005).: IEEE.

[Palmgren, 1924] Palmgren, A. (1924). Die Lebensdauer von Kugellagern. *Zeitschrift des Vereins Deutscher Ingenieure*, 68(14), 339–341.

[Pao & Johnson, 2009] Pao, L. Y. & Johnson, K. E. (2009). A tutorial on the dynamics and control of wind turbines and wind farms. In *2009 American Control Conference (ACC)* (pp. 2076–2089).: IEEE.

[Popov, 2010] Popov, V. (2010). *Contact mechanics and friction: physical principles and applications*. Springer Science & Business Media.

[Radaj & Vormwald, 1995] Radaj, D. & Vormwald, M. (1995). Ermüdungsfestigkeit. *Grundlagen für Leichtbau, Maschinen-und Stahlbau*.

[Riziotis & Voutsinas, 2000] Riziotis, V. A. & Voutsinas, S. G. (2000). Fatigue loads on wind turbines of different control strategies operating in complex terrain. *Journal of Wind Engineering and Industrial Aerodynamics*, 85(3), 211–240.

[Rotea, 2014] Rotea, M. A. (2014). Dynamic programming framework for wind power maximization. In *Proc. 19th IAFC World Congress*, volume 19 (pp. 3639–3644).

[Rychlik, 1987] Rychlik, I. (1987). A new definition of the rainflow cycle counting method. *International Journal of Fatigue*, 9(2), 119–121.

[Schepers & Van der Pijl, 2007] Schepers, J. & Van der Pijl, S. (2007). Improved modelling of wake aerodynamics and assessment of new farm control strategies. In *J. of Physics: Conf. Series*, volume 75 (pp. 012039).: IOP Publishing.

[Sears et al., 1982] Sears, F. W., Zemansky, M. W., & Young, H. D. (1982). *University physics*. Addison-Wesley.

[Skogestad & Postlethwaite, 2007] Skogestad, S. & Postlethwaite, I. (2007). *Multivariable feedback control: analysis and design*. Wiley New York.

[Slootweg & Kling, 2003] Slootweg, J. & Kling, W. (2003). Is the answer blowing in the wind? In *IEEE Power and energy magazine* (pp. 26–33).

[Slootweg et al., 2011] Slootweg, J., Veldman, E., & Morren, J. (2011). Sensing and control challenges for smart grids. In *Proc. of the 2011 IEEE Conf. on Networking, Sensing and Control (ICNSC)*.

[Sloth et al., 2011] Sloth, C., Esbensen, T., & Stoustrup, J. (2011). Robust and fault-tolerant linear parameter-varying control of wind turbines. *Mechatronics*, 21(4), 645–659.

[Soleimanzadeh & Wisniewski, 2011] Soleimanzadeh, M. & Wisniewski, R. (2011). Controller design for a wind farm, considering both power and load aspects. *Mechatronics*, 21(4), 720–727.

[Soltani et al., 2011] Soltani, M., Wisniewski, R., Brath, P., & Boyd, S. (2011). Load reduction of wind turbines using receding horizon control. In *Control Applications (CCA), IEEE International Conf. on* (pp. 852–857).

[Sucuoğlu & Erberik, 2004] Sucuoğlu, H. & Erberik, A. (2004). Energy-based hysteresis and damage models for deteriorating systems. *Earthquake Engineering & Structural Dynamics*, 33(1), 69–88.

[Swierczynski et al., 2011] Swierczynski, M., Teodorescu, R., & Rodríguez, P. (2011). Lifetime investigations of a lithium iron phosphate (lfp) battery system connected to a wind turbine for forecast improvement and output power gradient reduction.

[Tawarmalani & Sahinidis, 2002] Tawarmalani, M. & Sahinidis, N. V. (2002). *Convexification and global optimization in continuous and mixed-integer nonlinear programming: theory, algorithms, software, and applications*, volume 65. Springer Science & Business Media.

[Torrisi & Bemporad, 2004] Torrisi, F. D. & Bemporad, A. (2004). HYSDEL-a tool for generating computational hybrid models for analysis and synthesis problems. *IEEE Transactions on Control Systems Technology*, 12(2), 235–249.

[Tyson & Novak, 2001] Tyson, J. J. & Novak, B. (2001). Regulation of the eukaryotic cell cycle: molecular antagonism, hysteresis, and irreversible transitions. *Journal of Theoretical Biology*, 210(2), 249–263.

[van der Hoven, 1957] van der Hoven, I. (1957). Power spectrum of horizontal wind speed in the frequency range from 0.0007 to 900 cycles per hour. *Journal of Meteorology*, 14(2), 160–164.

[Visintin, 1994] Visintin, A. (1994). *Differential models of hysteresis*. Springer Berlin.

[Willems, 1972] Willems, J. C. (1972). Dissipative dynamical systems part I: General theory. *Archive for Rational Mech. and Analysis*, 45(5), 321–351.

[Wisniewski & Leth, 2011] Wisniewski, R. & Leth, J. (2011). Convenient model for systems with hystereses-control. In *50th IEEE Conference on Decision and Control and European Control Conference (CDC-ECC)* (pp. 6140–6145).

[Zhou & Li, 2000] Zhou, X. Y. & Li, D. (2000). Continuous-time mean-variance portfolio selection: A stochastic LQ framework. *Applied Mathematics & Optimization*, 42(1), 19–33.

Contributions

SUMMARY

How can fatigue-damage for control of wind turbines be represented? Fatigue-damage is indeed a crucial factor in structures such as wind turbines that are exposed to turbulent and rapidly changing wind flow conditions. This is relevant both in their design stage and during the control of their operation. Accordingly, the most recognized methods of fatigue-damage estimation are discussed in this thesis.

In wind energy conversion systems there is an intrinsic trade-off between power generation maximization and mechanical load minimization. Due to this compromise of competing objectives, the inclusion of fatigue-damage within feedback control loops is of special interest.

Four strategies in total are proposed in this work: three for the wind turbine level and one for the wind farm level. On one hand, the three strategies in the turbine level are based on hysteresis operators and strive to reduce the damage in the drive-train. On the other hand, the wind farm level strategy addresses its mixed-objective operation, allowing the wind farm to balance its power production and infrastructure wear, depending on what is more important.

This thesis adds findings to the current insight of fatigue-damage estimation in wind turbine components, to the mixed objective operation of wind energy conversion systems, and to the synthesis of control strategies that include hysteresis operators.

ISSN (online): 2246-1248
ISBN (online): 978-87-7112-398-2

AALBORG **UNIVERSITETSFORLAG**